

INFERENTIAL MODEL PREDICTIVE CONTROL
OF
POLY(ETHYLENE TEREPHTHALATE) DEGRADATION
DURING EXTRUSION

A THESIS SUBMITTED TO
THE GRADUATE SCHOOL OF NATURAL AND APPLIED SCIENCES
OF
MIDDLE EAST TECHNICAL UNIVERSITY

BY

MURAT OLUŞ ÖZBEK

IN PARTIAL FULFILLMENT OF THE REQUIREMENTS
FOR
THE DEGREE OF MASTER OF SCIENCE
IN
CHEMICAL ENGINEERING

AUGUST 2006

Approval of the Graduate School of Natural and Applied Sciences.

Prof Dr. Canan Özgen
Director

I certify that this thesis satisfies all the requirements as a thesis for the degree of Master of Science.

Prof. Dr. Nurcan Baç
Head of Department

This is to certify that we have read this thesis and that in our opinion it is fully adequate, in scope and quality, as a thesis for the degree of Master of Science.

Assoc. Prof. Dr. Göknur Bayram
Co-supervisor

Prof. Dr. Canan Özgen
Supervisor

Examining Committee Members

Prof. Dr. Güngör Gündüz (METU, CHE)_____

Prof. Dr. Canan Özgen (METU, CHE)_____

Doç Dr. Göknur Bayram (METU, CHE)_____

Doç. Dr. Naime Aslı Sezgi (METU, CHE)_____

Prof. Dr. Kemal Leblebicioğlu (METU, EE)_____

I hereby declare that all information in this document has been obtained and presented in accordance with academic rules and ethical conduct. I also declare that, as required by these rules and conduct, I have fully cited and referenced all material and results that are not original to this work.

Name, Last name:

Signature :

ABSTRACT

INFERENCEAL MODEL PREDICTIVE CONTROL OF POLY(ETHYLENE TEREPHTHALATE) DEGRADATION DURING EXTRUSION

Özbek, Murat Oluş

M. S., Department of Chemical Engineering

Supervisor: Prof. Dr. Canan Özgen

Co-Supervisor: Assoc. Prof. Dr. Göknur Bayram

August 2006, 91 pages

Poly(ethylene terephthalate), PET, which is commonly used as a packaging material, is not degradable in nature. As an issue of sustainable development it must be recycled and converted into other products. During this process, extrusion is an important unit operation. In extrusion process, if the operating conditions are not controlled, PET can go under degradation, which results in the loss of some mechanical properties.

In order to overcome the degradation of recycled PET (RPET), this study aims the control of the extrusion process. Dynamic models of the system for control purposes are obtained by experimental studies. In the experimental studies, screw speed, feed rate and barrel temperatures are taken as process variables in the ranges of 50 – 500 rpm, 3.85 – 8.16 g/min and 270 – 310 °C respectively. Singular value decomposition (SVD) technique is used for the best pairing between the manipulated – controlled variables, where screw speed is taken as the manipulated variable and molecular weight of the product is taken as the controlled variable. PID and model predictive controller (MPC) are designed utilizing the dynamic models in the feedback inferential control algorithm. In the simulation studies, the performance of the designed inferential control system, where molecular weight (M_w) of the product is estimated from the measured intrinsic viscosity ($[\eta]$) of the product, is investigated.

The controller utilizing PID and MPC control algorithms are found to be robust and satisfactory in tracking the given set points and eliminating the effects of the disturbances.

Keywords: extrusion, modeling, MPC, inferential control, PET recycling.

ÖZ

EKSTRÜZYON İŞLEMİNDE POLY(ETİLEN TEREFTALAT) BOZUNMASININ ALGISAL MODEL ÖNGÖRÜMLÜ DENETLEÇ İLE DENETLENMESİ

Özbek, Murat Oluş

Yüksek Lisans, Kimya Mühendisliği Bölümü

Tez Yöneticisi: Prof. Dr. Canan Özgen

Ortak Tez Yöneticisi: Doç. Dr. Göknur Bayram

Ağustos 2006, 91 sayfa

Genellikle, paketlenme malzemesi olarak kullanılan polietilen tereftalat'ın (PET) doğada bozunma özelliği yoktur. Bu nedenle, sürdürülebilir gelişme sürecinde PET'in geri kazanılması ve yararlı ürünlere dönüştürülmesi gerekir. Bu işleme süreçlerinde ekstrüzyon yöntemi önemli bir temel işlemdir. Ancak, ekstrüzyon sürecinde koşulların iyi ayarlanamadığı durumlarda, PET, bozunmaya (degradation) uğrayabilir ve bunun sonucunda mekanik bazı özelliklerini kaybedebilir.

Bu çalışmada, PET'in bozunmasının önlenmesi için ekstrüzyon sürecinin denetimi amaçlanmıştır. Denetimde kullanılmak üzere, sistemin dinamik modelleri deneysel çalışmalar yardımıyla elde edilmiştir. Deneysel çalışmalarda süreç değişkenleri olarak 270 - 310 °C aralığında kovan sıcaklığı (T), 50 – 500 dev/dak aralığında vida hızı (SS), 3.85 - 8.16 g/dak aralığında besleme oranı (FR) seçilmiştir. En iyi ayarlanan-denetlenen değişken eşleştirmesi için Tekil Değer Ayrıştırma (SVD) tekniği kullanılmış ve ayarlanan değişken olarak vida hızı (SS), denetlenen değişken olarak ürünün molekül ağırlığı (M_v) seçilmiştir. Elde edilen dinamik modellerle geleneksel (PID) ve model öngörümü denetleçler (MÖD) tasarlanmış ve geri beslemeli, algısal denetim algoritmasında kullanılmıştır. Benzetim çalışmalarında, ürünün molekül ağırlığının (M_v) ölçülen içsel viskozite ($[\eta]$) değerlerinden tahmin edildiği algısal denetim yapısının performansı incelenmiştir.

PID ve MÖD denetim algoritmaları kullanan denetleçlerin hem gürbüz hem de ayar noktası izleme ve bozan etkenin etkisini uzaklaştırma konularında başarılı oldukları irdelenmiştir.

Anahtar Sözcükler: ekstrüzyon, modelleme, model öngörümlü denetim, algısal denetim, geri dönüşümlü PET.

Dedicated to all my beloved ones...

ACKNOWLEDGMENTS

First of all, I wish to express my sincere gratitude to my supervisor Prof. Dr. Canan Özgen and co-supervisor Assoc. Prof. Göknuur Bayram for their valuable suggestions, guidance and understanding throughout my graduate study.

I would like to thank to all of my colleagues; especially to Salih Obut, Almıla Bahar, İsmail Doğan, Hatice Ceylan, Sertan Yeşil, Güralp Özkoç, Işıl Işık, Özcan Köysüren and Mert Kılınc for their help and support during my graduate study.

I would like to thank to all my co-workers in Middle East Technical University Graduate School of Natural and Applied Sciences for their support and understanding.

Last but not least, I wish to express my deepest thanks to my family for their great support, encouragement, and patience throughout my all education.

TABLE OF CONTENTS

PLAGIARISM	iii
ABSTRACT	iv
ÖZ	vi
ACKNOWLEDGMENTS.....	ix
TABLE OF CONTENTS.....	x
LIST OF TABLES.....	xii
LIST OF FIGURES.....	xiv
NOMENCLATURE.....	xvii
CHAPTER	
1. INTRODUCTION.....	1
2. LITERATURE SURVEY	3
2.1 Extrusion, Extruder Modeling and Extruder Control.....	3
2.2 PET Recycling and PET Degradation	8
2.3 Model Predictive Control (MPC)	10
2.4 Inferential Control	12
2.5 Singular Value Decomposition (SVD)	13
3. BACKGROUND INFORMATION ON PET AND CONTROL TECHNIQUES	14
3.1 Poly(ethylene terephthalate) (PET).....	14
3.1.1 Recycling.....	15
3.1.2 Degradation.....	16
3.2 Control Techniques	18
3.2.1 MPC	18
3.2.1.1 MPC Algorithm.....	18
3.2.1.2 Constrained MPC	20
3.2.3 Inferential Control	21
3.3 Singular Value Decomposition (SVD)	22
4. EXPERIMENTAL STUDIES.....	24
4.1 Properties of rPET and Trifluoroacetic Acid (TFA)	24
4.2 Experimental Setup	25
4.3 Experimental Procedure.....	27

4.3.1 Preliminary Experiments	27
4.3.2 Steady State Experiments	28
4.3.3 Dynamic Experiments	29
5. RESULTS AND DISCUSSIONS	31
5.1 Preliminary Experimental Results	31
5.2 Steady State Experimental Results	33
5.3 Dynamic Experimental Results	36
5.4 Modeling Studies	39
5.4.1 Modeling Technique 1: Single Transfer Functions	41
5.4.2 Modeling Technique 2: Dual Transfer Functions	44
5.4.3 Modeling Technique 3: Discrete Convolution Models	46
5.5 Control Studies	49
5.5.1 Singular Value Decomposition	49
5.5.2 Design of Control Scheme	51
5.5.3 PID Control	52
5.5.4 Model Predictive Control (MPC)	54
5.5.4.1 Process Models for MPC	54
5.5.4.2 MPC Tuning	55
5.5.5 Robustness Analysis	63
6. CONCLUSIONS	72
REFERENCES	73
APPENDICES	
A. MOLECULAR WEIGHT DETERMINATION	77
B. CALIBRATION FOR RESIDENCE TIME AND FEED RATE	79
C. EXPERIMENTAL DATA	82
D. PID CONTROL LOOP AND PROGRAM CODES	84
E. SAMPLE CALCULATIONS	88

LIST OF TABLES

TABLES

Table 3.1: Minimum requirements for RPET flakes to be reprocessed [Ajawa and Pavel, 2005].	16
Table 4.1: Properties of RPET resin (AdvanSA).	25
Table 4.2: Step changes given to the process variables.	29
Table 5.1: Measured intrinsic viscosity and molecular weight of unprocessed RPET.	32
Table 5.2: Results of consistency check	36
Table 5.3: Single transfer function models and their normalized IAE scores.	42
Table 5.4: Dual transfer function models and their normalized IAE scores.	44
Table 5.5: PID settings utilizing modified Z-N method (Some Overshoot) [Seborg et al., 1989], and normalized IAE scores of set point tracking (Figure 5.19).	52
Table 5.6: Fine tuned PID settings for PID^+ and PID^- .	53
Table 5.7: The magnitudes and the time of changes of the given set point changes.	54
Table 5.8: MPC tuning parameters.	56
Table 5.9: Normalized IAE scores of controllers throughout set point tracking.	57
Table 5.10: Normalized IAE scores and settling times of controllers in disturbance rejection performances.	60
Table 5.11: Normalized IAE scores of controllers throughout set point tracking (10% increase in model gains).	65
Table 5.12: Normalized IAE scores of controllers throughout set point tracking (10% decrease in model gains).	65
Table 5.13: Normalized IAE scores and settling times of controllers in disturbance rejection performances (10% increase in model gains).	70
Table 5.14: Normalized IAE scores and settling times of controllers in disturbance rejection performances (10% decrease in models gains).	71
Table B.1: Average residence times for studied screw speeds.	79
Table B.2: Flow rate calibration data for studied feed rate settings.	80
Table C.1: Molecular weight (g/gmol), M_v , change for different SS and FR values at 270 °C.	82
Table C.2: Molecular weight (g/gmol), M_v , change for different SS and FR values at 290 °C.	82

Table C.3: Molecular weight (g/gmol), M_v , change for different SS and FR values at 310 °c.	82
Table C.4: M_v (g/gmol) change with SS, FR and T (dynamic runs).....	83
Table E.1: Experimental data (an example).....	88
Table E.2: Reduced viscosity for different concentrations.....	89
Table E.3: Ultimate gains and ultimate periods of positive and negative PID-model pairs....	90
Table E.4: Original and modified Ziegler-Nichols settings for PID controllers [Seborg et al., 1989].	91

LIST OF FIGURES

FIGURES

Figure 3.1: PET synthesis reactions: (a) trans-esterification reaction and (b) condensation reaction [Ajawa and Pavel, 2005].	15
Figure 3.2: Thermal degradation of PET [Karayannidis et al., 2000].	17
Figure 3.3: Acid alcohol condensation of PET [Karayannidis and Psalida, 2000].	17
Figure 3.4: Open loop step response of a linear plant [Seborg et al., 1989].	18
Figure 3.5: Block diagram for inferential control loop.	21
Figure 4.1: Molecular formula of trifluoroacetic acid (TFA).	24
Figure 4.2: Extruder used for experiments.	26
Figure 4.3: Schematic drawing for the experimental setup.	26
Figure 4.4: Control panel of the extruder (a: die temperature and pressure, b: melt temperatures, c: barrel temperatures, d: screw speed and torque, e: main feed rate).	27
Figure 5.1: The effect of temperature on molecular weight of RPET.	32
Figure 5.2: Effect of SS and FR on M_v at $T = 270$ °C.	34
Figure 5.3: Effect of SS and FR on M_v at $T = 290$ °C.	34
Figure 5.4: Effect of SS and FR on M_v at $T = 310$ °C.	35
Figure 5.5: System responses to (a) positive (+25 rpm) and (b) negative (-50 rpm) steps on screw speed.	37
Figure 5.6: System responses to (a) positive (+1.04 g/min) (+25) and (b) negative (-1.42 g/min) (-25) steps on feed rate.	38
Figure 5.7: System responses to (a) positive (+20 °C) and (b) negative (-20 °C) steps on temperature.	38
Figure 5.8: Model representation of the system.	40
Figure 5.9: Plant and model responses to a (a) positive and (b) negative unit step changes in SS (single transfer function case).	41
Figure 5.10: Plant and model responses to a (a) positive and (b) negative unit step changes in FR (single transfer function case).	43
Figure 5.11: Plant and model responses to a (a) positive and (b) negative unit step changes in T (single transfer function case).	43

Figure 5.12: Plant and model responses to a (a) positive and (b) negative unit step changes in SS (dual transfer functions case).	45
Figure 5.13: Plant and model responses to a (a) positive and (b) negative unit step changes in FR (dual transfer functions case).	45
Figure 5.14: Plant and model responses to a (a) positive and (b) negative unit step changes in T (dual transfer functions case).	46
Figure 5.15: Plant and model responses to a (a) positive and (b) negative unit step changes in SS (discrete convolution models case).	47
Figure 5.16: Plant and model responses to a (a) positive and (b) negative unit step changes in FR (discrete convolution models case).	48
Figure 5.17: Plant and model responses to a (a) positive and (b) negative unit step changes in T (discrete convolution models case).	48
Figure 5.18: Designed control system.	52
Figure 5.19: Set point tracking of PID controllers of (a) positive and (b) negative models, tuned using modified Z-N settings (Some Overshoot) [Seborg et al., 1989].	53
Figure 5.20: Responses of ARX models to (a) positive and (b) negative unit step changes in SS.	55
Figure 5.21: Set point tracking responses of PID and MPC.	56
Figure 5.22: Disturbance rejection responses of PID and MPC (+25 or +1.04 g/gmol step disturbance on FR).	57
Figure 5.23: Disturbance rejection responses of PID and MPC (-25 or -1.42 g/gmol step disturbance on FR).	58
Figure 5.24: Disturbance rejection responses of PID and MPC (+10 °C step disturbance on T).	59
Figure 5.25: Disturbance rejection responses of PID and MPC (-10 °C step disturbance on T).	59
Figure 5.26: Disturbance rejection responses of PID and MPC (+12.5 or +0.57 g/gmol step disturbance on FR).	61
Figure 5.27: Disturbance rejection responses of PID and MPC (-12.5 or -0.71 g/gmol step disturbance on FR).	61
Figure 5.28: Disturbance rejection responses of PID and MPC (+20 °C step disturbance on T).	62
Figure 5.29: Disturbance rejection responses of PID and MPC (-20 °C step disturbance on T).	62
Figure 5.30: Set point tracking responses of PID and MPC (10% increase in model gains). ..	64
Figure 5.31: Set point tracking responses of PID and MPC (10% decrease in model gains). ..	64

Figure 5.32: Disturbance rejection responses of PID and MPC (+1.04 g/gmol step disturbance on FR) (10% increase in model gains).	66
Figure 5.33: Disturbance rejection responses of PID and MPC (-1.42 g/gmol step disturbance on FR) (10% increase in model gains).	66
Figure 5.34: Disturbance rejection responses of PID and MPC (+1.04 g/gmol step disturbance on FR) (10% decrease in model gains).	67
Figure 5.35: Disturbance rejection responses of PID and MPC (-1.42 g/gmol step disturbance on FR) (10% decrease in model gains).	67
Figure 5.36: Disturbance rejection responses of PID and MPC (+10 °C step disturbance on T) (10% increase in model gains).	68
Figure 5.37: Disturbance rejection responses of PID and MPC (-10 °C step disturbance on T) (10% increase in model gains).	69
Figure 5.38: Disturbance rejection responses of PID and MPC (+10 °C step disturbance on T) (10% decrease in model gains).	69
Figure 5.39: Disturbance rejection responses of PID and MPC (-10 °C step disturbance on T) (10% decrease in model gains).	70
Figure A.1: Ostwald and Ubbelohde viscometers.	78
Figure B.1: Average residence times measured at different screw speeds.	80
Figure B.2: Feed rate settings and corresponding flow rates (g/min).	81
Figure D.1: Feedback control loop for PID controllers designed in SIMULINK.	84
Figure E.1: Reduced viscosity change with concentration.	90

NOMENCLATURE

a	Step response coefficient
A	Coefficient matrix
E	Error
E	Error vector
FR	Feed Rate (g/gmol)
G	Steady-state gain matrix
h	Impulse response coefficient
K	Gain matrix
K	Gain value or Mark-Hauwing constant
L	Control horizon
m	Manipulated variable
M	Input vector
M_v	Viscosity average molecular weight
M_w	Weight average molecular weight
PP	Polypropylene
r	Set point
R	Prediction horizon
SS	Screw Speed (rpm)
T	Temperature ($^{\circ}$ C)
U	Left singular matrix in SVD
V	Right singular matrix in SVD
y	Output
Y	Output vector
Subscripts:	
n	Sample number (in means of Δt)
Superscripts:	
c	Corrected prediction
d	Desired value
p	Predicted value
N	Normalized value

Greek Letters:

α	Filter value or Mark-Hauwing constant
λ	Weighting matrix diagonal element
τ	Process transfer function time constant
Δ	Increment
ω	Weighting matrices
$[\eta]$	Intrinsic viscosity
η_{red}	Reduced viscosity
η_{rel}	Relative viscosity
Σ	Sum or Singular value matrix in SVD

Abbreviations:

ANN	Artificial Neural Network
ARTD	Average Residence Time Distribution
DMC	Dynamic Matrix Control
ILR	In-line reometer
IMC	Internal Model Control
IV	Intrinsic Viscosity
LDPE	Low Density Polyethylene
MAC	Model Algorithmic Control
MFI	Melt Flow Index
MI	Melt Index
MIMO	Multiple Input Multiple Output
MPC	Model Predictive Control
MPHC	Model Predictive Heuristic Control
MVC	Minimum Variance Conroller
PET	Poly(ethylene terephthalate)
PVC	Polyvinyl chloride
RPET	Recycled poly(ethylene terephthalate)
RTD	Residence Time Distribution
SISO	Single Input Single Output
SSE	Single Screw Extruder
STR	Self Tuning Regulator
SVD	Singular Value Decomposition
TFA	Trifluoroacetic acid
TSE	Twin Screw Extruder

CHAPTER I

INTRODUCTION

PET, which is a thermoplastic resin of polyester family, has become one of the major packaging materials due to its good barrier and mechanical properties. Due to its non-degradable nature, PET must be recycled for sustainable development and must be used to obtain other byproducts. Today, PET is one of the most recycled materials world wide.

The major drawback in PET recycling is the loss of the molecular weight, a phenomenon known as degradation. Heat, mechanical effects, contaminants and water moisture are the important factors of degradation. Degradation has an adverse effect on the mechanical properties of the product. Therefore, degradation amount should be reduced to preserve the mechanical properties. Molecular weight can be used to express the degradation amount.

Extruders are commonly used machinery in plastics processing and recycling industries. Previous studies [Incarnato et al., 2000; Spinace et al., 2000; Assadi et al., 2004; Ajawa and Pawel, 2004] showed that the degradation of RPET is caused mainly by processes taking place in the extruder. Furthermore, the quality of an extruded product is directly related to its rheological properties such as melt viscosity of the material in the extruder. Thus, extrusion process should be controlled in order to reduce the degradation amount.

Previous studies [Parnaby et al., 1975; Smith et al., 1978; Hassan and Parnaby, 1981, Costin et al., 1982; Yang and Lee, 1986; Tanttu et al., 1989; Pabendiskas et al., 1989; Nied et al., 2000; Xiao et al., 2001; Previdi et al., 2006] on the control of an extruder or extrusion process mainly focused on regulating the process parameters like screw speed, barrel temperatures or barrel/die temperature or pressure on defined preset values. However, in such a regulation, expert knowledge on the operation and on the relations between the process conditions and product properties is required. In order to eliminate the requirement of such an expert knowledge, by using the secondary measurements, an inferential control

scheme can be designed for the control of desired product property whose online measurement is not possible.

Product property is important for the downstream operations of the extruder and can be kept constant at a desired point by designing a proper control mechanism for the extruder. Among the different types of controllers, model predictive controller (MPC) has proven itself worthy and being used in the industry for the last two decades. Although different algorithms exist for MPC, the name basically refers to a family of controllers in which the future behavior of the plant is predicted using a dynamic model of the plant and necessary control actions are calculated in an optimal manner.

In this study, the control of product quality in terms of molecular weight of extruded RPET is aimed. The system parameters affecting the molecular weight (M_v) are screw speed (SS), feed rate (FR) and temperature (T). Thus the inputs are considered to be SS, FR and T, and the output as M_v . The die temperature, die pressure and torque which are additional parameters are not taken as variables in the scope of this study. Nominal operating point in term of SS, FR and T, suitable for fiber production is determined by using the steady state experimental data. Dynamic experiments are conducted to obtain the relations between the inputs (SS, FR and T) and the output (molecular weight of the extruded product) of the extruder. These data are used to obtain the dynamic models of the process. An inferential control scheme is designed to control the molecular weight of the product for different disturbances by simulation studies by using dynamic models. In the designed control scheme, performances of PID and MPC controllers are studied.

The outline of this work is as follows. A literature survey on previous studied on related subjects is given in Chapter 2. Background information about PET and control techniques are given in Chapter 3. Experimental studies including the set-up and procedures are summarized in Chapter 4. Chapter 5 includes the results of all the experimental, modeling and control studies with discussions. Conclusions are given in the last chapter, Chapter 6.

CHAPTER II

LITERATURE SURVEY

PET is one of the commonly recycled industrial plastics. However, in order to overcome the phenomenon of losing material property during recycling, one option is to control the process to obtain a product with desired property. Control of product property in an extrusion process is a challenging one as the aimed product property cannot be measured online in most of the cases. This problem can be overcome by building an inferential control scheme by measuring the viscosity of the product on-line and predicting the molecular weight from this measurement. Furthermore, using a model based controller seems promising to yield more successful results. A literature survey about these subjects is presented in this chapter.

2.1 Extrusion, Extruder Modeling and Extruder Control

Parnaby et al. (1975) studied the automatic control of an extruder. Their work mainly outlines the basics of the development of a feed-forward adaptive predictive control strategy. Also system identification and modeling were done such as stochastic identification techniques, step and impulse models. The basic structure for the extruder control scheme and the interaction between the extruder and the die variables were illustrated. In their work screw speed was accepted as the manipulated variable and the die pressure, as a measure of degree of mixing, which indirectly gives the product quality, as the controlled variable. The melt temperature was also monitored to understand the dynamics better. It is also stated that by on-line updating the model, small changes in model can be compensated.

Smith et al. (1978) explained the operating characteristics of twin screw extruders (TSE). The study focused on the interrelationships between the design parameters (such as screw design, die geometry, feed zone geometry), material properties, and operation variables

(such as screw speed, barrel and die temperatures). The effects of these variables and parameters on the product and product quality during operation are also reviewed. In the work, first, the effects of the parameters were explained mathematically under certain assumptions. Finally, these parameter based mathematical models were illustrated for control purposes. Neither experimental nor simulation studies were carried out. Only the responses to changes in screw speed and feed rate were illustrated using the obtained models.

Hassan and Parnaby (1981) experimentally constructed a cascade (hierarchical) control loop on a laboratory scale extruder and studied the feed-back and feed-forward control strategies. The constructed system measured barrel and die wall temperatures and pressures, screw speed and the 'restrictor valve' position on the die. Measuring these, the control system sent set points to screw speed, die restrictor valve, barrel and die wall temperatures. To achieve this goal, the controller used the constructed model of the extruder and die behavior, and an optimization function to calculate the control action. Also, in the work two aims of the extruder control are specified as set point tracking (steady-state control) and disturbance rejection (dynamic control).

Costin et al. (1982) published a review on the present literature about the dynamic modeling and control of plasticizing extruder. They developed the subject into three headings, which were extruder disturbance studies, classical control studies and stochastic control studies. It was pointed that the previous works were mainly focused on long-term disturbances related with the melt temperature, melt pressure or extrudate thickness.

Costin et al. (1982) studied the effects of the screw speed on the die pressure and temperature. System dynamics were modeled as first order with dead time and time series models. Die pressure was controlled by manipulating screw speed. The disturbance was introduced to the system as difference in feed material composition. Digital PI, self tuning regulator (STR) and minimum variance controllers (MVC) were studied and compared. The results of the study showed that instead of eliminating the disturbances, the STR tuned itself to eliminate the flight noise, which is caused due to the rotation of the screw.

Yang and Lee (1986) proposed several feedback and feed-forward control methods to control long term and short term disturbances and evaluated these methods using various load changes. The aim was to control the extrudate thickness by manipulating the take-up speed against the screw speed load. A first order model was developed and PI controller

with Smith predictor and digital noise filters were tested for load and set-point changes. The experimental results showed that the control structure was good at set-point changes but its performance was low at load changes due to the inaccuracy of the model.

Tanttu et al. (1989) planted STR on extruder in simulation level in order to control the start-up period of the extruder by regulating the barrel temperatures. For mathematical description of the system a distributed parameter model was used. For parameter estimation different algorithms were tested. The simulation results showed that STR can be used with a proper parameter estimation algorithm for the start-up and normal operation.

Pabendinskas et al. (1989) studied the degradation of polypropylene (PP) in a reactive extrusion process to produce PP with a specified molecular weight (M_w). The measured and manipulated variables were die pressure drop and initiator concentration, respectively. The initiator (peroxide) concentration was manipulated via syringe pump. Online measured viscosity via die pressure drop, and melt flow index (MFI), measured via online rheometer, were used to determine the amount of degradation. Step tests were performed to find the relation between the die pressure drop and degradation, and this relation was modeled with a first order with dead time model. The implemented controller scheme was consisted of a gain scheduling controller with Smith dead time compensator and a PI controller. The PI controller was used in a cascade manner to control the syringe pump. The results of the study indicated that the desired M_w could be achieved by the control of the pressure drop.

Boadhead et al. (1996) developed an in-line rheometer (ILR), which had a 'partial Couette' geometry, to reduce the measurement delay, and described its use. The reactive extrusion process was modeled as a first order with dead time process. PI and minimum variance controllers were tested. The results showed that there was a considerable dead time in spite of the ILR advantages. It is also offered that the use of adaptive techniques for such a system could improve the controller performance, because the tested controllers' performances were not good due to the non-linearity of the process.

De Ruyck (1997) developed a residence time distribution (RTD) model for a twin screw food extruder. The model was constructed as series of CSTRs with recycling flows and different volumes. Effects of the variables (screw profile, screw speed, water supply, feed supply and die diameter) on RTD were observed experimentally and compared with the model results and seen to be in agreement. By using the model the effect of different screw designs were also studied.

Elsay et al. (1997) developed a dynamic model that predicts the variables affecting the product quality in a single screw food extruder. The model was fitted to experimental data and it was used in an inferential control algorithm. PI and MPC controllers were tested on simulation level. MPC results came out to be much better than that of PI controller.

Nield et al. (2000) constructed a two input two output MIMO MPC scheme with constraints, to control the product property (weight average molecular weight (M_w) and high molecular weight end of molecular weight distribution) of LDPE in a reactive extrusion process by manipulating the width and amplitude of square peroxide waves. The product property of LDPE was inferred by using the measurements of an 'inline wedge rheometer'. The controller scheme was tested on actual plant. The results showed that, the control of consistency index was good however power law index was not, due to the imposition of input constraints, tuning of the controller for slow closed loop response and ill conditioning of the system.

Haley and Mulvaney (2000) implemented a non-linear MPC on a food extruder in a cascade manner. The objective was to obtain the product with the minimum piece density with the constraint, where the other quality attributes should be acceptable. Responses of 'specific mechanical energy (SME)' to screw speed and feed rate were modeled. Operating point set points were obtained by an inferential model. In the cascade strategy, MPC was placed on the inner loop and the cascade controller on the outer loop. Also a ratio controller was utilized in a feed-forward manner to control the moisture content, and to eliminate the disturbances in the feed. Furthermore the whole scheme was supplied with a feedback algorithm on output, which corrects the model errors and disturbances. The results showed that the scheme performed well for both disturbance rejection and set point tracking.

Wang and Tan (2000) developed a 'dual-target predictive control strategy', which could track both the input and output set points in an optimal manner and applied to food extruder. Die pressure and die temperature were the constructed model's inputs and screw speed, feed rate and moisture addition were the outputs. The case which the both input and output set-points can be followed was called as 'realizable case' and the results showed that the controller achieved its goal for this case.

Xiao et al. (2001) studied the control of coating properties of low-density polyethylene (LDPE). The controlled and manipulated variables were the melt strength and the screw

speed respectively. The melt strength was measured by passing the extrudate through a pulley system connected to a balance. The disturbance was introduced by changing the type of LDPE fed, while the feed rate was kept unchanged. The PI and MPC were tuned offline and their on-line performances were tested individually. In the work it was pointed that there is a high order relation between the input and the output, which resulted in MPC's better performance.

Lee et al. (2002) tried to improve a previous work on the same subject where a blockage phenomenon encountered in a food extruder. In order to prevent this phenomenon screw speed was controlled by fuzzy reasoning. The fuzzy inputs were screw speed percentage and torque percentage and the manipulated variables were water and feed flow and screw speed and torque percentages. The study achieved its goal and the blockage was prevented.

Chen et al. (2003) proposed an 'empirical viscosity model for quality control in the polymer extrusion process'. In this work the viscosity was calculated using the parameters; screw speed, melt temperature, geometric dimensions of the extruder and experimentally determined material constants. The method was offered as an alternate and to overcome the disadvantages of in-line capillary rheometer. The results of the work showed that the proposed models can be applied to the product quality control using viscosity as the main control parameter in the polymer extrusion process without implementing an in-line rheometer, which would influence the output of the product.

Mudalamane and Bigio (2003) developed a first principles model and studied the effects of external disturbances on the output fluctuations and transient behavior of extruders. Based on the previous work, disturbances were categorized as high, medium and low frequency disturbances. By using the model, damping effects of extruder design parameters on these disturbances were studied. The simulation studies showed that, for a given screw design, the process had a characteristic critical frequency above which the disturbances with higher frequencies were damped out, however the ones with lower frequencies were not.

Choulak et al. (2004) developed a dynamic model for reactive extrusion in a twin screw extruder, that predicted pressure, filling ratio, temperature and molar conversion. The model was built as series of CSTRs that could be partially filled or fully filled with back flow. Validation of the model was carried out by comparing the simulation data and the experimental data. A good agreement between these data sets was observed. Aim of

automatic control of polymerization conditions in a twin screw extruder was mentioned but no control studies were carried out.

Wang et al. (2004) presented a 'three-stage approach to system identification in the continuous time'. The three stages are; data acquisition using relay feedback, non-parametric identification of the system step response, and parametric model fitting of the identified step response. In the work discrete time noise model was integrated into continuous time system identification. Experimental results were obtained by applying the proposed method on a pilot scale food extruder and the results were presented in comparison with model data.

Previdi et al. (2006) experimentally tested a prototype feedback control system for the control of volumetric flow in a single screw extruder. The manipulated variables were the barrel temperatures and die pressure. The work presents all the steps of the controller from modeling to experimental testing. The results of the tests showed that the control scheme responded well to disturbance rejections with small offsets on temperature and pressure.

2.2 PET Recycling and PET Degradation

Tanrattanakul et al. (1996) studied 'toughening of PET by blending with a functionalized polystyrene-poly(ethylene-co-butylene)-polystyrene (SEBS) block copolymer'. The aim was to increase fracture strain that was affected by both blend composition and degradation caused by process conditions. The processes utilized were extrusion and injection molding. The intrinsic viscosity of PET was measured by Ubbelohde type viscometer using 60w/40w phenol/tetrachloroethane as solvent. Results showed that the blending increased the fracture strain of PET. Torres et al. (2001) also made a similar study. They tried to improve the thermal and mechanical properties of PET and recycled PET using chain extenders. They also used the same solvent and equipment type for solution viscosity measurements.

Incarnato et al. (2000) aimed to increase the M_w of recycled PET to make it suitable for film blowing and blow molding, by using pyromellitic dianhydride (PDMA) as chain extender, in a single step reactive extrusion. Effect of PDMA content on molecular structure was investigated by using different concentrations of chain extenders, and then the extruded PET samples were characterized. Results showed that a certain amount of PDMA increased M_w and branching, broadened M_w/M_n , making recycled PET suitable for film blowing and blow

molding. Awaja and Davier (2004) made a similar study on an industrial scale extruder, where PET was recycled by PDMA chain extender. In this work, effects of residence time and temperature were also studied.

Pawlak et al. (2000) made a study on the 'characterization of scrap PET' in order to find methods of characterization of recycled polymers and to show 'general tendencies in property change'. Applied techniques to achieve this goal were; differential scanning calorimetry (DSC), Fourier transform infrared spectroscopy (FTIR), thermogravimetry (TGA), dilute solution viscometry and dynamic viscosity measurement via capillary die. In the work, it was pointed out that the main problem in polymer recycling was the segregation, which was caused by the impurities that catalysis hydrolysis. In the study, scrap PET from beverage bottles were obtained from different sources, and extruded in a laboratory scale single screw extruder. Results showed that the presence of more than 50 ppm PVC made PET unsuitable for more advanced processes such as film blowing.

Spinace et al. (2000) processed the PET used for production of soft drink bottles for five times using SSE, and characterized rheological, mechanical and thermal properties of the product including carboxylic end group number and melt flow index (MFI) analysis. The study showed that after three processing cycles, changes in the crystallinity degree and in the mechanical properties were occurred. It was pointed that the increase in MFI and carboxylic end group concentration was a sign of mechanical degradation. The experiments showed that the temperature profile changes were more affective using low screw speed, which shows that the residence time has a direct affect on polymer degradation. Another result of the study was that even after five processing cycles, thermal degradation behavior of PET did not change.

Chelsea Center For Recycling And Economic Development (University of Massachusetts), published the results of their laboratory study about "potential end uses for polyester fiber waste", on their technical report no.33 (2000). The PET fiber wastes were extruded using different compositions of materials such as PET bottle waste, glass fiber and polycarbonate. Products of these different compositions were tested separately with and without further processing like molding. The effects of different factors, such as processing conditions, presence of impurities and additive types, on the product's quality and properties were discussed.

Oromiehie and Mamizadeh (2004) studied PET beverage bottle recycling and methods to improve its properties. The aim was to process and modify the mixture of virgin and recycled grade PETs, with and without chain extender (PP-graft-MA) by different extrusion methods and then to characterize the samples. Determination of tensile and thermal properties, viscosity and M_w , and impact tests were carried out. Results showed that the intrinsic viscosity ($[\eta]$) decreased as thermal process cycles and amount of recycled PET concentration increased. Also, the chain extender improved the properties of the blends.

Assadi et al. (2004) studied the degradation types of PET during recycling by extrusion. The experiments were performed using scraps of post-consumer PET, in a single screw extruder at different temperatures. The M_w of the extruded samples were determined using steric exclusion chromatography (SEC), rheological tests and infrared measurements (IR). The experiments were carried out using nitrogen and air environments with different air pressures. A kinetic model for PET degradation was built, and results obtained from the model were compared with the experimental ones. This comparison showed that model results were in good match for nitrogen and oxygen environments.

Ajawa and Pawel (2005) made a brief review of PET recycling, taking the subject starting from the synthesis of virgin PET, its properties, processing and applications. Use of chain extenders was discussed, with the available machinery such as extruders to overcome the molecular weight loss problem during recycling. Finally, to convert the RPET to a valuable product, processes such as injection stretch blow molding (ISBM), which is a way to produce PET bottles, were reviewed.

2.3 Model Predictive Control (MPC)

Marchetti et al. (1983) described the basics of a predictive control algorithm that was based on discrete convolution models. Developed SISO predictive controller was compared to a PID controller for three process models on simulation levels, and for an experimental continuous stirred tank heater. Although predictive controller was superior on simulations, a significant improvement was not observed in the experimental system. However, it was pointed that the real advantage of predictive controllers was for MIMO cases.

Maurath et al. (1989) discussed the effects of the controller design parameters on closed loop performance and robustness for an unconstrained SISO linear process. A stability

analysis that considers the plant/model mismatch was developed. Effects of design parameters on controller's performance were illustrated on several examples.

Brengel and Seider (1989) developed a model predictive algorithm for nonlinear MIMO case. The control actions were calculated with a multi step predictor by linearizing ODEs. The proposed algorithm was capable of easily handling of input and output constraints. In simulation studies, the multi step predictor out performed the single step predictor.

Garcia et al. (1989) published a survey paper about MPC and compared several predictive controller algorithms such as DMC, MAC and IMC. They pointed that the significant advantage of MPC was the 'flexible constraint handling capability'. Applications of MPC on nonlinear systems were also investigated and concluded that the adjustment of MPC was easier although it was not more robust than conventional feed-back controllers.

Morningred et al. (1992) developed an adaptive nonlinear controller similar to standard linear model predictive controller. In the algorithm the number of tuning parameters could be reduced to one. For the developed algorithm, effects of the modeling errors were shown, and it was compared to PI, adaptive linear predictive controller and non-adaptive nonlinear predictive controller, on a CSTR model. Results showed that the controller was computationally efficient and could perform well even initially designed with modeling errors.

Meziou et al. (1996) used a dynamic CSTR model of an ethylene-propylene-diene polymerization reactor to simulate the servo and regulatory performance of three input three output MIMO DMC. Polynomial equations that relate the process's gains to the magnitude of the input change were derived, because the amplitude of the change in the input caused variations in the gains of the process. Simulation results showed that the capability of MIMO DMC to reduce the off-spec product amount caused by the set point changes and/or disturbances.

Özkan et al. (2003) controlled the polymerization reaction in a CSTR with the developed MPC algorithm that different linear models instead of a non-linear model. The objective function included finite and infinite horizon cost components. The finite component made the system move towards the desired operating point and the infinite component, having an upper bound, brought the system to desired steady state operating point. Simulation results showed that the proposed controller was successful at achieving the control goals.

Biagiola et al. (2005) published their case study about 'use of state estimation for inferential non-linear MPC'. The proposed non-linear estimator updates the state vector and estimates the unmeasured disturbances where feed concentration was not measured. In the algorithm concentration was inferred via temperature measurements. In simulation studies the proposed non-linear observer non-linear controller structure is found to have good performance to reject disturbances even in the presence of significant disturbance variations and noisy measurements.

2.4 Inferential Control

Doyle III (1998) published a review in which inferential control, linear and non-linear estimation techniques like moving horizon estimation methods or linearization by output injection were presented and discussed. New theoretical approaches were presented on a simple chemical reactor example.

Ogawa et al. (1999) built an inferential control scheme to control the melt index (MI) of the product of a HDPE process. The MI was estimated by using the measurements of feed and co-catalyst concentration and temperature measurements. The constructed inferential model was based on a previous work of writers, simplifying it by means of computational burden. The calculation of the control law was based on the relations of inferential model. The system showed good regulatory and set point tracking responses on an industrial polyolefin production.

Wang et al. (2001) implemented an inferential MPC algorithm on a food extruder, where screw speed was manipulated variable and the bulk density of the product was controlled variable, in order to control the product quality. The work also demonstrates the building a continuous time dynamic model based on multi-rate sampled data. Experimental application of the algorithm showed that the inferential control system maintains the product quality within the specific ranges.

Bahar et al. (2004) utilized MPC to build an inferential control loop of an industrial multi component batch distillation column. The MIMO MPC controlled the product compositions in a feed-back manner, using the estimated values of the product compositions coming from the artificial neural network (ANN) estimator. The estimator used the temperature measurements from the selected trays. Simulation results showed that the unconstrained

and constrained MPC performances using ANN estimator, could be alternative to the controller using direct composition values.

2.5 Singular Value Decomposition (SVD)

Klema and Laub (1980) have given a descriptive introduction to the singular value decomposition (SVD) from the point of view of its computation and potential applications. They emphasized certain important details of the implementation of SVD on a digital computer. They also included a number of illustrative examples and computed solutions, and concluded that singular value analysis forms a fundamental basis of modern numerical linear algebra.

Rojas et al. (2004) proposed a strategy for the solution of quadratic performance index of the optimal control law with constraints on inputs. A MIMO system whose Hessian of the performance index had a large condition number was chosen for the illustration. Sub-optimal control laws were obtained using SVD on Hessian matrix. Proposed strategy was compared against MPC. Although the results were similar, proposed strategy held the advantage of requiring no solution to the quadratic programming problem.

Zheng and Hoo (2004) used SVD technique to reduce the order of a distributed parameter system (DPS). The system at hand was a tubular reactor, which was modeled as time series model (infinite order). Order of this dynamic model was reduced to 3rd order in temperature and 1st order in concentration. This linear model was then used as the plant model in a quadratic dynamic model based controller (QDMC) and results were illustrated.

Luyben (2006) quantitatively compared the effectiveness of five different criteria for selecting the temperature control trays in a distillation column. Their effectiveness were tested on several systems ranging from ideal binary to azeotropic multi-component. Results showed that among the tested criteria, SVD analysis provides a simple and effective method for selecting tray locations.

CHAPTER III

BACKGROUND INFORMATION ON PET AND CONTROL TECHNIQUES

The detailed information about PET (synthesis, recycling and degradation), control techniques (MPC and inferential control) and SVD analysis used in the study are given below.

3.1 Poly(ethylene terephthalate) (PET)

PET is a thermoplastic resin of polyester family. It was patented in 1941 and was commercially introduced as a textile fiber in 1953. The first PET bottle was patented in 1973.

PET has become a very important packaging material due to its good barrier and mechanical properties. It makes a good barrier to gas, to alcohol (requires additional treatment) and to many of the solvents. Furthermore semi-crystalline PET presents good thermal and mechanical properties such as high melting temperature (approximately 250 °C).

PET can be synthesized by trans-esterification and/or condensation reactions as shown in Figure 3.1. Depending on its processing conditions, amorphous (transparent) or semi-crystalline (opaque and white) PET can be obtained.

The bulk synthesis of PET is carried out at 270 to 285 °C, with continuous removal of gas to pressure below 1 mm Hg. The removal of methanol or water increases the molecular weight of the polymer. If the methanol or the water were left in the same system, they would cause a reverse reaction which would cause depolymerization.

The polymerization of PET can be carried out in the presence of a catalyst such as Sb, Ba, Ca, Cd, Co, Pb, Mn, Mg, Ti, and Zn.

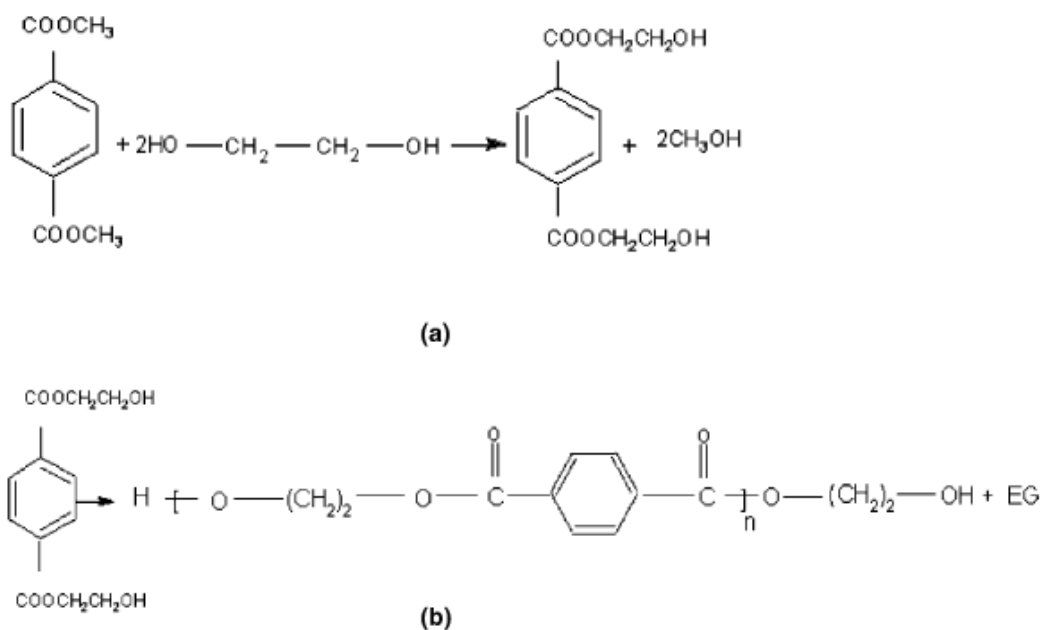


Figure 3.1: PET synthesis reactions: (a) trans-esterification reaction and (b) condensation reaction [Ajawa and Pavel, 2005].

3.1.1 Recycling

PET recycling is the activity in which “post-consumer PET” or “recycled PET (RPET)”, mainly formed of the collected beverage bottles, is reprocessed to a valuable product.

PET is non-degradable in nature, and its recycling is forced by environmental laws. Furthermore, post-consumer PET is cheaper than virgin (non-processed) PET. For these reasons PET recycling represents one of the most successful and widespread example of polymer recycling. Today, approximately 1.5 million tons of PET is collected worldwide per year. Petcore, the European trade association that fosters the collection and recycling of PET, forecasts that in Europe alone, collection will exceed one million tons by 2010 [petcore.org].

During thermal recycling process, mechanical effects, moisture and presence of impurities (PVC, adhesives, dyes, etc.), cause the loss of molecular weight (*degradation*) and lead to a decrease in intrinsic viscosity ($[\eta]$), resulting in decrease in mechanical properties. RPET having an intrinsic viscosity about 0.60 dl/g would be appropriate for fiber production, 0.65 dl/g for film production, 0.76 dl/g for bottle production and 0.85 dl/g for tire cord production [Chelsea Center For Recycling And Economic Development, 2000].

RPET should satisfy the specifications given in Table 3.1 to be used as raw material.

Table 3.1: Minimum requirements for RPET flakes to be reprocessed [Ajawa and Pavel, 2005].

Property	Value
Intrinsic viscosity ($[\eta]$)	> 0.7 dl/g
Melting temperature (T_m)	> 240 °C.
Water content	< 0.02 wt.%
Flake size	0.4 mm < D < 8 mm
Dye content	< 10 ppm
Yellowing index	< 20
Metal content	< 3 ppm
PVC content	< 50 ppm
Polyolefin content	< 10 ppm

3.1.2 Degradation

PET undergoes thermal, mechanical and hydrolytic chain scissions during recycling. Polymer chains break by giving the volatile products mainly terephthalic acid, acetaldehyde and carbon monoxide. A sample reaction is given in Figure 3.2.

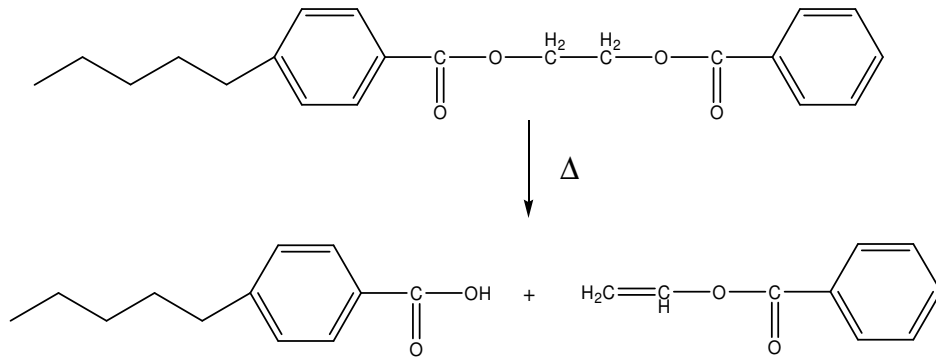


Figure 3.2: Thermal degradation of PET [Karayannidis et al., 2000].

Mechanical degradation occurs due to the physical effects such as shear stress applied by the extruder screws.

Hydrolytic degradation can be seen as the major effect reducing the molecular weight. This type of chain scission is catalyzed by the impurities readily present in RPET, such as water moisture, PVC, acid producing elements, dyes, etc. Acid alcohol condensation, catalyzed by water is given in Figure 3.3 as an example. Hydrolytic degradation can be reduced by drying the PET prior to processing.

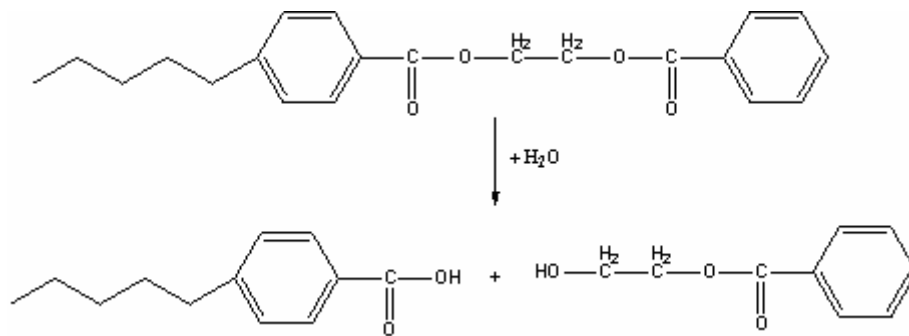


Figure 3.3: Acid alcohol condensation of PET [Karayannidis and Psalida, 2000].

3.2 Control Techniques

In the control of the extruder system (see Chapter 4) MPC and PID techniques using inferential models are used. A summary on MPC control technique and inferential control will be given below.

3.2.1 MPC

Beginning from the late 1970's predictive control techniques such as 'Model Algorithmic Control (MAC)' [Richlet et al., 1978] (also known as Model Predictive Heuristic Control or MPH) or 'Dynamic Matrix Control (DMC)' [Cutler and Ramaker, 1980] began to gain importance with the improving computer technology. Up to now, predictive control techniques proved their efficiencies in many applications.

Although different MPC algorithms utilize different computation techniques, all utilize the previous knowledge about plant dynamics (*plant model*) to predict what the plant output will be after a definite time (*prediction horizon*), and calculates the next n number of control actions (*control horizon*) in an *optimal* manner.

3.2.1.1 MPC Algorithm

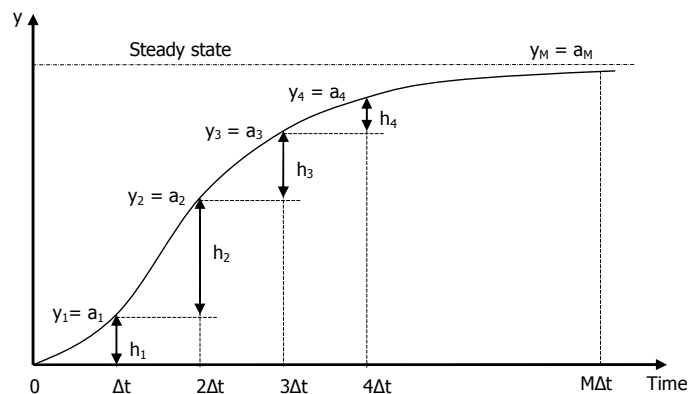


Figure 3.4: Open loop step response of a linear plant [Seborg et al., 1989].

In the MPC algorithm, future projection of the plant is calculated using the *step response coefficients* (see Figure 3.4) in Equation 3.1 [Marchetti, 1981].

$$\mathbf{E}^P = -\mathbf{A}^T \Delta \mathbf{m} + \hat{\mathbf{E}}^P$$

$$\begin{bmatrix} y_{n+1}^d - y_{n+1}^c \\ y_{n+2}^d - y_{n+2}^c \\ \vdots \\ y_{n+R}^d - y_{n+R}^c \end{bmatrix} = - \begin{bmatrix} a_1 & a_2 & \cdots & a_R \\ 0 & a_1 & \cdots & \vdots \\ \vdots & \vdots & \ddots & a_2 \\ 0 & 0 & 0 & a_1 \end{bmatrix} \begin{bmatrix} \Delta m_n \\ \Delta m_{n+1} \\ \vdots \\ \Delta m_{n+R-1} \end{bmatrix} + \begin{bmatrix} (1-\alpha^1)E_n - P_1 \\ (1-\alpha^2)E_n - P_2 \\ \vdots \\ (1-\alpha^R)E_n - P_R \end{bmatrix} \quad (3.1)$$

where subscript R denotes the *prediction horizon* and n denotes the sampling instant. The superscript c denotes the corrected prediction and d denotes the desired value. The letters y , m , a and E are used to represent the *plant output*, *plant input*, *step response coefficients* and *error* respectively. The predicted errors, P , are calculated as follows.

$$P_l = \sum_{k=1}^l \left(\sum_{i=k+1}^R h_i \Delta m_{n+k-i} \right) \quad (3.2)$$

$$k, l = 1, 2, \dots, R$$

If a perfect match between the predicted and the desired values is wanted ($\mathbf{E}^P = 0$) then, from Equation 3.1 the control action can simply be calculated as,

$$\Delta \mathbf{m} = (\mathbf{A}^T)^{-1} \hat{\mathbf{E}}^P \quad (3.3)$$

Equation 3.3 gives the control action at present sampling instant by predicting the next R number of plant output. By applying the first element of $\Delta \mathbf{m}$ vector and repeating the procedure at every sampling instant the plant output is kept on desired values. But this control law does not come out to be satisfactory as it tries to force the output to the desired value at one sampling instant. To overcome this problem two proposed approaches are Model Algorithmic Control (MAC) [Mehra et al., 1982; Richalet et al., 1978] and Dynamic Matrix Control (DMC) [Cutler and Ramaker, 1980].

DMC reduces the dimension of $\Delta \mathbf{m}$ from R (prediction horizon) to L (control horizon), and only L number of future control actions are calculated. Thus, Equation 3.1 can be rewritten as,

$$\mathbf{E}^P = -\mathbf{A} \Delta \mathbf{m} + \hat{\mathbf{E}}^P \quad (3.4)$$

\mathbf{A} being the $\mathbf{R} \times \mathbf{L}$ "Dynamic Matrix" equal to the first \mathbf{L} columns of \mathbf{A}^T . Optimal solution of Equation 3.4 is obtained by minimizing the performance index by least squares. The solution for the control action gives,

$$\Delta \mathbf{M} = (\mathbf{A}^T \mathbf{A})^{-1} \mathbf{A}^T \hat{\mathbf{E}}^p \quad (3.5)$$

"One difficulty with the above control law is that if the $\mathbf{A}^T \mathbf{A}$ matrix is ill conditioned it can result in large changes in the manipulated variable (ringing) or even unstable process" [Marchetti, 1983]. This problem can be eliminated by introducing "weighting matrices" \mathbf{W}_1 and \mathbf{W}_2 , which limit the manipulated variable moves, to the performance index.

$$\mathbf{J}(\Delta \mathbf{M}) = (\mathbf{E}^p)^T \mathbf{W}_1 \mathbf{E}^p + \Delta \mathbf{M}^T \mathbf{W}_2 \hat{\mathbf{E}}^p \quad (3.6)$$

which results in the following control law:

$$\Delta \mathbf{M} = (\mathbf{A}^T \mathbf{W}_1 \mathbf{A} + \mathbf{R})^{-1} \mathbf{A}^T \mathbf{W}_2 \hat{\mathbf{E}}^p \quad (3.7)$$

Here, again, the first control action is applied and new control law is calculated by observing the plant output at each step. As only the first control action, Δm_n is applied, the control law can be reduced to,

$$m_n = m_{n-1} + \mathbf{K}^T \hat{\mathbf{E}}^p \quad (3.8)$$

where elements of \mathbf{K}^T (*gain matrix*), are the elements of the first row of $(\mathbf{A}^T \mathbf{A})^{-1} \mathbf{A}^T$ in Equation 3.5.

3.2.1.2 Constrained MPC

Up to this point no constraints are taken into account in the calculation of the control law. However, in most processes, constraints should be imposed to the control actions, due to the physical limitations and/or safety margins of the plant. Constraints may also be placed to the plant output in order to prevent high deviations on product quality. When the constraints are introduced, then the solution of the objective function becomes an optimization problem in the following form:

$$\begin{aligned} \min \quad & \mathbf{J}(\Delta\mathbf{M}) = (\mathbf{E}^p)^T \mathbf{W}_1 \mathbf{E}^p + \Delta\mathbf{M}^T \mathbf{W}_2 \hat{\mathbf{E}}^p \\ \text{subject to:} \quad & \\ & \Delta m_{\min} \leq m_n - m_{n-1} \leq \Delta m_{\max} \\ & m_{\min} \leq m_n \leq m_{\max} \\ & y_{\min} \leq y_n \leq y_{\max} \end{aligned} \tag{3.9}$$

3.2.3 Inferential Control

In order to build a feed-back control algorithm, regardless of the controller type, on-line measurement of the controlled output(s) is required. However, in quite a large number of chemical process applications direct on-line measurement of the controlled output is late, expensive or not available at all, which are the cases that limits the construction of the feed-back control scheme [Seborg et al., 1989]. Feed-forward control could be utilized in such cases being limited to the presence of measured disturbances and an appropriate model. For the cases where neither on-line measurement of output nor unmeasured disturbances is available, inferential control can be used to keep track of the unmeasured output. A block diagram of inferential control loop is given in Figure 3.5.

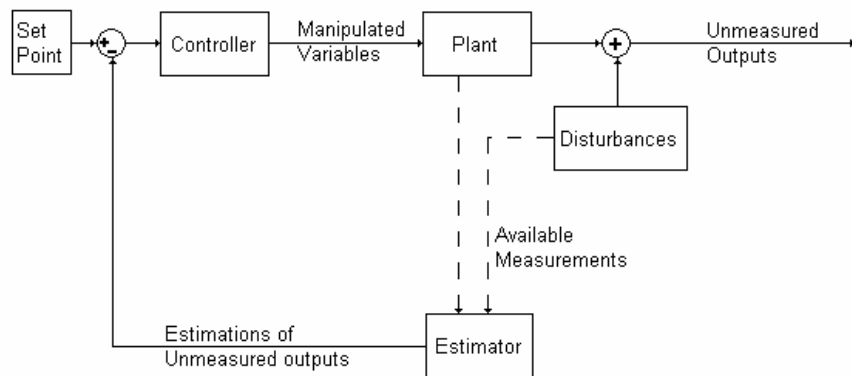


Figure 3.5: Block diagram for inferential control loop.

3.3 Singular Value Decomposition (SVD)

SVD is an extension of singular value analysis (SVA). It is used to determine the rank and condition of a matrix and also to determine the strengths and weaknesses of a set of equations [wikipedia.org]. In control point of view, SVD is utilized for controlled-manipulated variable pairing for a MIMO system. In the frame of this work, only control aspect of SVD will be given.

In the simplest form, SVD is the factorization of a rectangular matrix, as follows:

$$\mathbf{K} = \mathbf{U}\mathbf{\Sigma}\mathbf{V}^T \quad (3.10)$$

Where \mathbf{K} is the $m \times n$ matrix, \mathbf{U} is the $m \times m$ orthonormal matrix called *left singular matrix* that contains output basis vector directions for \mathbf{K} , $\mathbf{\Sigma}$ is an $m \times n$ diagonal matrix of *singular values* that can be thought as scalar gains, and \mathbf{V} is an $n \times n$ orthonormal matrix called *right singular matrix* that contains input basis vector directions for \mathbf{K} .

Steady state relations of a MIMO system, with n number of outputs and m number of inputs, can be expressed in vector-matrix form as:

$$\mathbf{Y} = \mathbf{G}\mathbf{M} \quad (3.11)$$

Where, \mathbf{Y} is the output vector, \mathbf{G} is the *steady state gain matrix* and \mathbf{M} is the input vector.

It is possible to find which output is sensitive to which input by applying SVD to \mathbf{G} . From the resulting \mathbf{U} and \mathbf{V} matrices, largest element of 1st column of \mathbf{U} (Δy_n) is most sensitive to the changes in the largest element of 1st column of \mathbf{V} (m_m), largest element of 2nd column of \mathbf{U} to the largest element of 2nd column of \mathbf{V} , etc.

For the cases where number of inputs and outputs of the system are not equal to each other, the pairings corresponding to the zero elements of $\mathbf{\Sigma}$ does not have to be calculated. Such a calculation is called as the *compact SVD*.

Another aspect of SVD is the *Condition Number*, CN. It is defined as the ratio of the largest and the smallest non-zero singular values:

$$CN = \frac{\sigma_l}{\sigma_r} \quad (3.12)$$

For a large CN of \mathbf{G} , the system is said to be ill-conditioned. Furthermore, if \mathbf{G} is singular, then it is ill-conditioned.

CHAPTER IV

EXPERIMENTAL STUDIES

In the experimental studies done, RPET is extruded at different processing conditions and samples are collected for molecular weight determination to obtain degradation data. Materials used, experimental procedure, setup and machinery are presented in this chapter.

4.1 Properties of RPET and Trifluoroacetic Acid (TFA)

RPET is used in the form of flakes in the experiments. The properties of the RPET as specified by the supplier (AdvanSA, Adana) are presented in Table 4.1.

Two commonly used solvents for PET are, 40wt% tetracholoro ethane – 60wt% phenol mixture and trifluoroacetic acid (TFA). Being carcinogenic, the first one is eliminated and TFA is used as the solvent. Figure 4.1 shows the molecular structure of TFA.

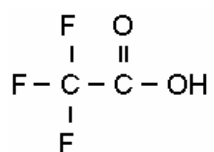


Figure 4.1: Molecular formula of trifluoroacetic acid (TFA).

Mark Hauwing constants for PET-TFA solution at 25 °C are $K = 14 \times 10^{-4}$ and $\alpha = 0.65$ [Brandrub and Immergut, 1989]:

Table 4.1: Properties of RPET resin (AdvanSA)

Contaminants (ppm)	PVC	60
	Polyethylene	5
	Metal pieces	0
	Adhesive	10
	Paper pieces	3
Lighting Characteristics	Value L, Shining	66.1
	Value B, Yellowness	2.6
	Value A, Redness	-2.0
Material Properties	Intrinsic Viscosity ($[\eta]$)	0.750 dl/g
	Glass Transition Temperature (T_g)	60 °C
	Melting Temperature (T_m)	255 °C – 260 °C

4.2 Experimental Setup

RPET is extruded using a laboratory scale co-rotating twin screw extruder (Thermoprism TSE 16TC, L/D = 24) as shown in Figure 4.2 to obtain degradation data. The schematic drawing for the extruder system is given in Figure 4.3.

The extruder had five electrical heaters through the barrel, whose temperatures can be set separately. The cooling is provided by passing through cooling water in the barrel. The feed is supplied via a brabender type feeder whose screw speed can be adjusted. The parameters that can be set from the control panel of the extruder are screw speed, feed rate (feeder screw speed), and temperatures of each 5 heating zones.

The available measurements from the control panel are screw speed, temperatures of each five heating zones, melt temperatures from four distinct points, die pressure and temperature. A photograph of the control panel is given in Figure 4.4.

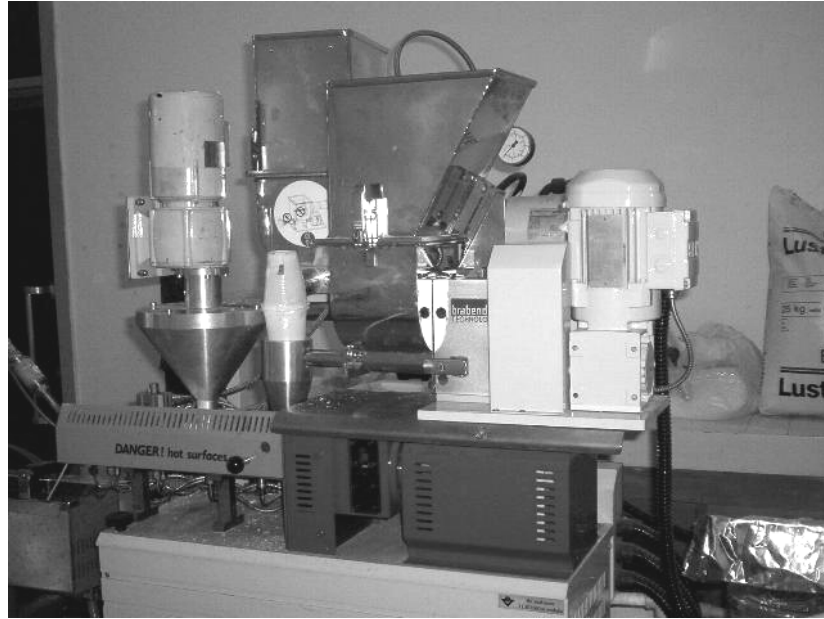


Figure 4.2: Extruder used for experiments.

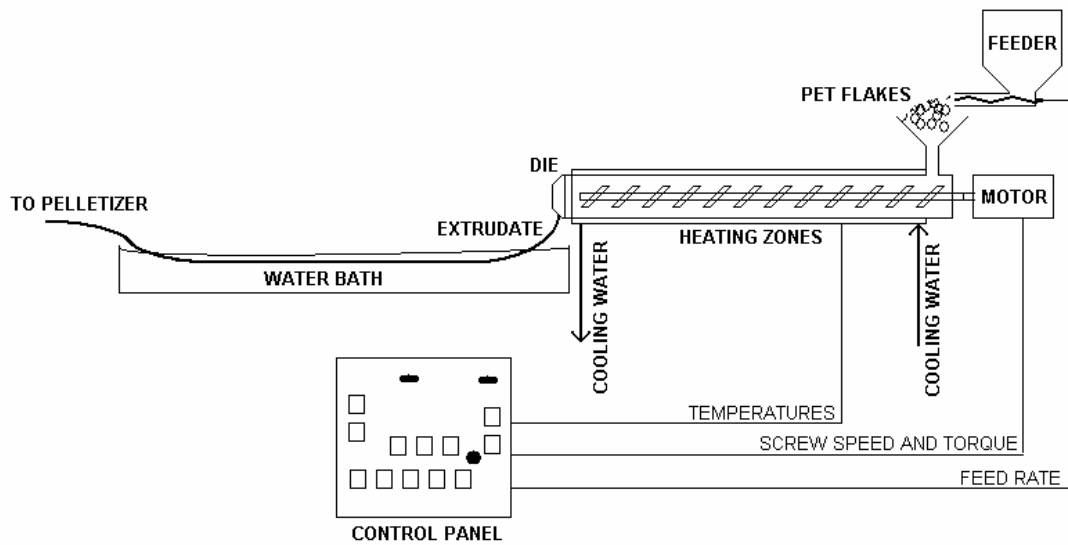


Figure 4.3: Schematic drawing for the experimental setup.

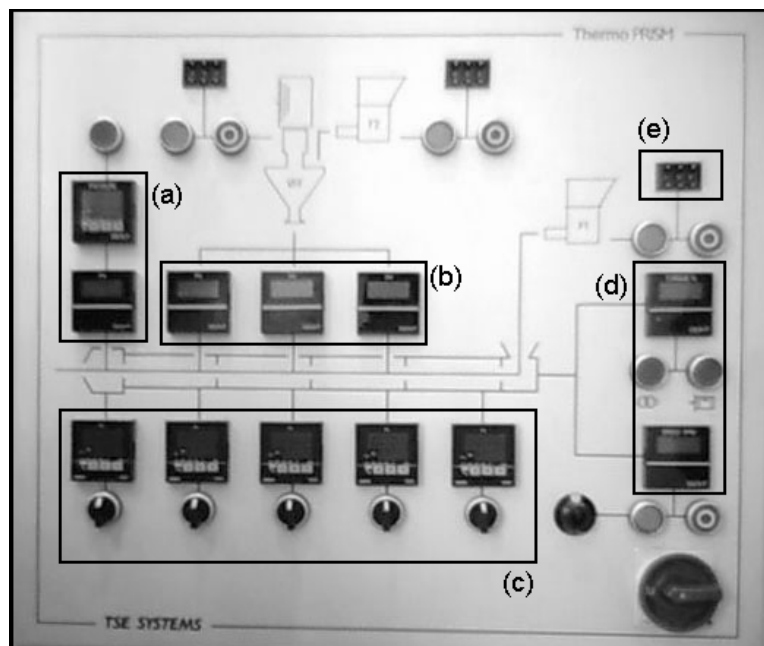


Figure 4.4: Control panel of the extruder (a: die temperature and pressure, b: melt temperatures, c: barrel temperatures, d: screw speed and torque, e: main feed rate).

4.3 Experimental Procedure

The experiments are carried out in two phases. In the first phase preliminary and steady state experiments are done and in the second phase dynamic experiments are carried out.

4.3.1 Preliminary Experiments

In the preliminary experiments the effect of temperature on viscosity and molecular weight is investigated. Also the calibration of the extruder is done.

Effect of Temperature: The effect of temperature on RPET degradation is studied by eliminating other parameters. Samples are packed firmly in aluminum foil and are held in oil bath at 4 different temperatures (270, 280, 290, 300°C) for 1, 3 and 5 minutes. The intrinsic viscosities ($[\eta]$) of these 12 samples are determined by dilute solution viscometry (see Appendix A).

The choice of studied temperature and time ranges are based on the studied temperature and residence time range of extrusion. The residence time range of the extrusion depends upon the screw speed in a twin screw extruder (see Appendix B). Thus in these experiments, effect of screw speed in means of residence time is also included indirectly. Auto ignition temperature of silicone oil limited the testing of higher temperatures.

Calibration of the Extruder: In order to find the flow rate (g/min) equivalent of feed rate setting of extruder control panel, the feed flow is collected for one minute intervals and weighted. Different feed rate settings such as 25, 50, 75 and 100, are used and average values for flow rates are found by repeating the experiments.

The residence times for the studied screw speeds (50, 125, 200, 275, 350, 425 and 500 rpm) are measured by using carbon-black containing polyethylene (PE) pellets as indicator. The indicator pellets are dropped manually into the feeding point while the main feed (RPET) is being fed. The time when the product color (originally semi-transparent or opaque white) changed from gray to black is recorded as the *average residence time* (ART).

4.3.2 Steady State Experiments

The aim of these experiments is to determine the intrinsic viscosities ($[\eta]$) and corresponding molecular weights (M_v) of products processed at different operating conditions.

RPET is extruded at 3 different temperatures¹, 270, 290 and 310 °C; 4 different feed rate settings, 25, 50, 75 and 100; and 7 different screw speeds, 50, 125, 200, 275, 350, 425 and 500 rpm, resulting in 84 samples.

After the system is reached its steady state operating conditions ($t \gg \text{ART}$) (see Appendix B) 25-30 grams of samples are collected from the extruded product. The samples are too

¹ The barrel temperatures' setting is a parameter itself for output properties. In this study, the temperature of each zone is set constant and equal to each other, to eliminate the effect of this parameter. For example, $T = 270 \text{ }^\circ\text{C}$ means that all the temperatures along the barrel are set to 270 °C.

thin and elastic to be pelletized in the pelletizer, thus they are cut into small pieces at hand to homogenize. From homogenized sample particles, 0.06 gram is weighed for intrinsic viscosity ($[\eta]$) measurements.

4.3.3 Dynamic Experiments

These experiments are aimed to collect the necessary data to model the dynamic response of the system output (M_v) to the changes in the process parameters (SS, FR and T). In other words aim is to find out the pattern that M_v follows from one operating condition to other.

Using the data obtained from steady state experiments, operating conditions are selected as SS = 100 rpm, FR = 7.12 g/min (feed rate setting = 75) and T = 270 °C, for a product having an intrinsic viscosity value of $[\eta] = 0.6$ dl/g, which is suitable for fiber production [Chelsea Center For Recycling And Economic Development, 2000].

Thus, step changes given in Table 4.2 are introduced one at a time starting from this operating point. Each step change is given after bringing the system to the initial steady-state operating point.

Table 4.2: Step changes given to the process variables.

Variable	Initial steady state value	Plus change	Minus change
Screw speed	100 rpm	25 rpm	50 rpm
Feed rate ¹	7.12 g/gmol	1.04 g/gmol	1.42 g/gmol
Temperature	270 °C	20 °C	20 °C

For screw speed and feed rate changes, the samples are collected at 10 second intervals, whereas samples are collected at 20 second intervals for temperature changes. This is because the system responded to the changes in temperature more slowly. The first sample

¹ It should be noted that, for step changes on feed rate, feed rate setting of the control panel are taken as the basis. Calibration data for the feed rate setting and the material flow rate can be found in Appendix C

(sample at $t = 0$) is collected at the time when the step change is introduced. For every sampling time, outcoming product is collected for 5 seconds. Then, these samples are broken into small pieces manually for homogenization and 0.06 gram of each sample is weighted for intrinsic viscosity measurement.

CHAPTER V

RESULTS AND DISCUSSIONS

The results of preliminary experiments for the verification of supplier data for RPET specifications and the experiments on the effect of temperature on degradation of PET are given below. These will be followed by the results of experiments on the extruder under steady-state and transient conditions. The results of simulation and modeling studies will be introduced with discussions.

5.1 Preliminary Experimental Results

Verification of Supplier's Data: The intrinsic viscosity ($[\eta]$) and viscosity average molecular weight (M_v) of RPET is measured without processing the RPET samples, in order to check with the supplier's data. The results of these experiments are given in Table 5.1.

It is found that the experimentally measured value for $[\eta] = 0.75$ and corresponding molecular weight value, $M_v = 18363$ g/gmol are in a very good agreement with the supplier's data with an error of + 0.001 dl/g in $[\eta]$ and + 26 g/gmol in M_v .

Effect of Temperature on RPET Degradation: As given in Chapter 4, these experiments are performed in oil bath where samples of RPET are exposed to temperature in the range of 270 - 300 °C for different time durations. The results in terms of M_v are given in Figure 5.1.

Table 5.1: Measured intrinsic viscosity and molecular weight of unprocessed RPET.

Sample No.	Intrinsic viscosity ($[\eta]$) (dl/g)	Viscosity average molecular weight (M_v) (g/gmol)
1	0.750	18363
2	0.747	18248
3	0.751	18401
Avarage	0.749	18337
Supplier Data	0.750	18363

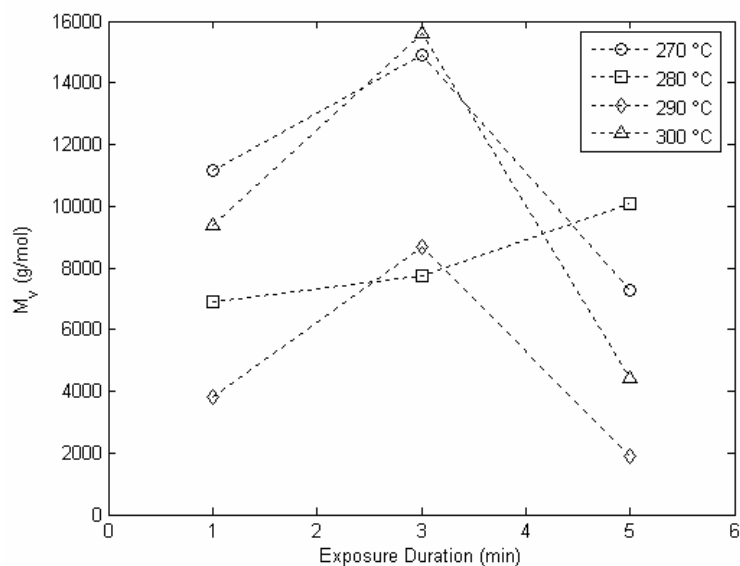


Figure 5.1: The effect of temperature on molecular weight of RPET.

Figure 5.1 shows that M_v does not follow a simple decreasing trend with increasing temperature with time. Instead, there exist some *optimal* points (or regions) where M_v increases and then decreases. Although not studied in this work, one possible cause may be the *branching* or *crosslinking*, which was also observed in the previous studies [Spinace et al., 2000; Pawlak et al., 2000; Assadi et al., 2004] on RPET degradation. It is known that heat causes the longer polymer chains break into smaller ones. In case of branching or crosslinking, these smaller chains form new bonds on the backbone of another chain, as a result of coupling alkyl radicals generated by the oxidation chain process, with the effect of

temperature [Assadi et al., 2004]. Furthermore, the contaminants of RPET, such as dyes and adhesives may have a catalyzing effect on this reaction.

Thus, it can be seen from Figure 5.1, M_v decrease within for temperatures 270, 290 and 300 °C. The only disagreement with this observation is the trend for 280 °C.

5.2 Steady State Experimental Results

Steady-state experiments with the laboratory scale co-rotating twin screw extruder are done in order to find the operating point which will produce an output with the desired intrinsic viscosity and molecular weight values of $[\eta] = 0.6$ dl/g and $M_v = 11500$ g/mol [Chelsea Center For Recycling And Economic Development, 2000]. A product with these values is suitable for the fiber production, one of the most important areas of use of the RPET.

Thus, RPET is extruded at three different barrel temperatures (270, 290 and 310°C), four different feed rates (3.85, 5.70, 7.12 and 8.16 g/min), and seven different screw speeds (50, 125, 200, 275, 350, 425 and 500 rpm). The viscosities of the samples from these 84 runs are measured to obtain the M_v relations as a function of process parameters. The results are given in Figures 5.2 to 5.4.

Figures 5.2 to 5.4 indicate that molecular weights of samples (see Appendix C) are as a function of screw speed at different temperatures and feed rates. The range of molecular weight of samples are approximately 2000 - 15000 for 270 °C, 6000 - 13000 for 290 °C, and 2000 - 11000 for 310 °C. These trends prove the degradation of M_v with temperature.

A similar generalization cannot be done for the effect of screw speed and feed rate on M_v . Shear stress exerted by the screws and the filling ratio, which is a function of both the screw speed and the feed rate are the two most probable effects on M_v degradation. The effect of filling ratio can be explained with the heat and shear consumed by unit amount of material in the extruder. Thus, oscillatory behavior of molecular weight can be due to the adverse effects of these two variables. Increasing the screw speed increases the shear stress applied and decreases the filling ratio, ending up in a decrease in M_v .

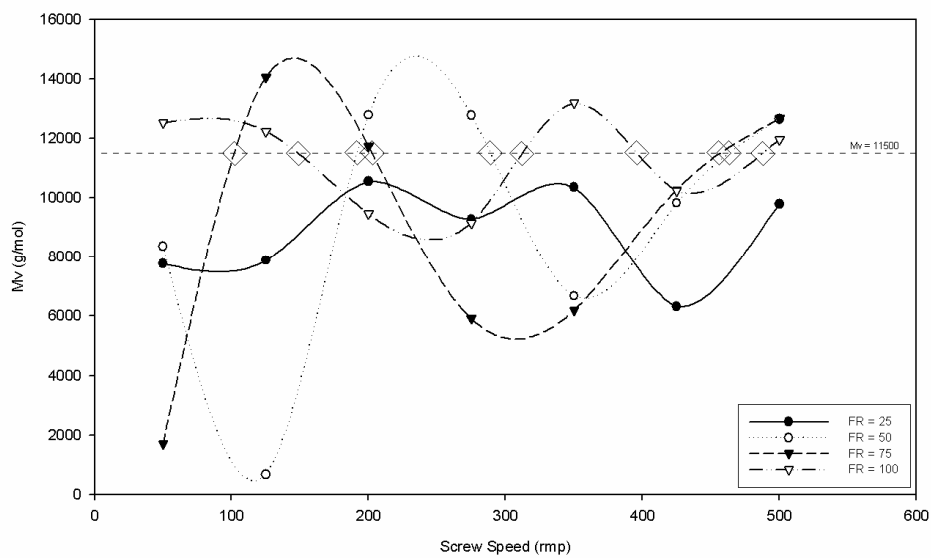


Figure 5.2: Effect of SS and FR on M_v at $T = 270$ °C.

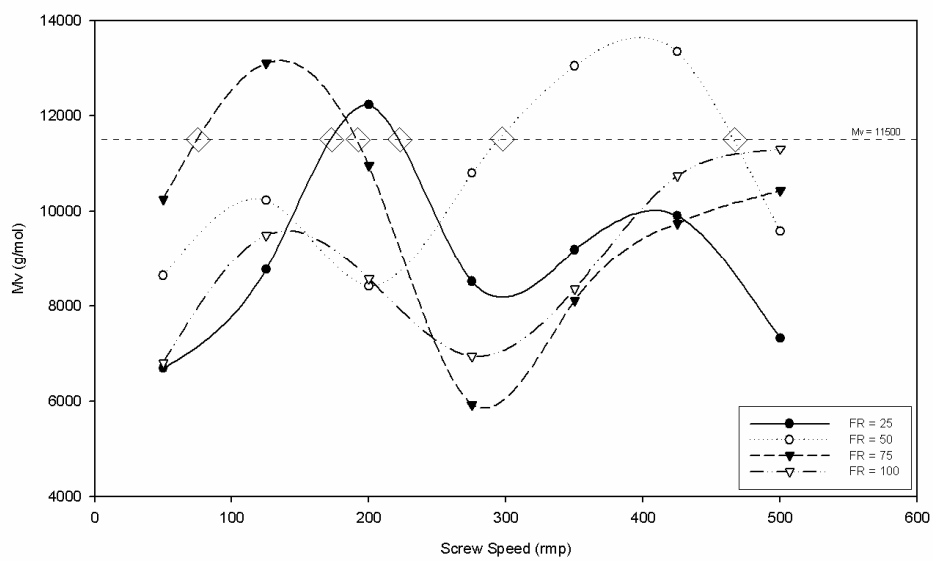


Figure 5.3: Effect of SS and FR on M_v at $T = 290$ °C.

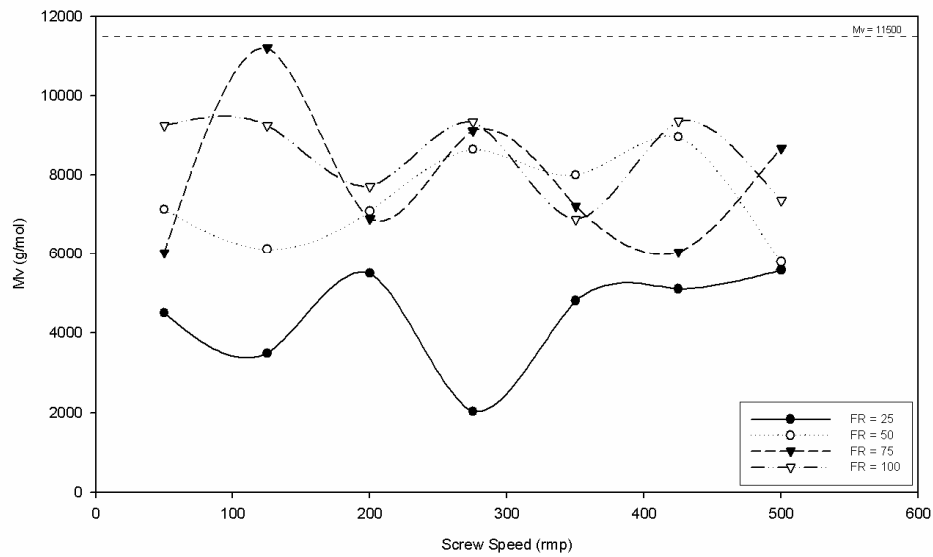


Figure 5.4: Effect of SS and FR on M_v at $T = 310\text{ }^\circ\text{C}$.

After the steady state measurements are completed, intrinsic viscosities of randomly selected nine samples are measured again to check the consistency of the previous measurements. As can be seen from Table 5.2, the precision of the measurements are acceptable.

In order to produce a product with a M_v of 11500 g/mol, it can be concluded from Figures 5.2 to 5.4 (\diamond marked points) that, this value can be obtained by the parameters $SS = 100$ rpm, $FR = 7.12$ g/min and $T = 270\text{ }^\circ\text{C}$. It is important to note that the operating point must be such that possible variations in the variables must not result in degradation in M_v . This is a required flexibility for a safe operation. If, for example, process temperature is chosen as $290\text{ }^\circ\text{C}$, then M_v for the product can only be achieved in a very restricted range. Due to large oscillation in the behavior of M_v as a function of SS and FR, at $T = 310\text{ }^\circ\text{C}$ $M_v = 11500$ g/mol cannot be obtained for any of the SS and FR values in the selected ranges.

Table 5.2: Results of consistency check

Sample from:	Previous measurement		Consistency measurement	
	$[\eta]$ (dl/g)	M_v (g/gmol)	$[\eta]$ (dl/g)	M_v (g/gmol)
T: 270 °C, FR: 25, SS: 200 rpm	0.526	10549	0.523	10221
T: 270 °C, FR: 75, SS: 125 rpm	0.632	14053	0.634	14123
T: 270 °C, FR: 100, SS: 500 rpm	0.570	11966	0.563	11731
T: 290 °C, FR: 25, SS: 50 rpm	0.393	6689	0.392	6657
T: 290 °C, FR: 50, SS: 425 rpm	0.614	13344	0.614	13426
T: 290 °C, FR: 100, SS: 500 rpm	0.550	11310	0.558	11565
T: 310 °C, FR: 25, SS: 200 rpm	0.350	5584	0.347	5497
T: 310 °C, FR: 25, SS: 200 rpm	0.479	9116	0.483	9241
T: 310 °C, FR: 25, SS: 200 rpm	0.484	9250	0.486	9307

5.3 Dynamic Experimental Results

The dynamic experiments which are aimed to find dynamic models for the process under the change of the manipulated variables and in the presence of disturbances are done with the changes of screw speed from 100 rpm to 125 rpm and from 100 rpm to 50 rpm, feed rate setting from 75 (7.12 g/min) to 100 (8.16 g/min) and from 75 (7.12 g/min) to 50 (5.70 g/min), barrel temperatures from 270 °C to 290 °C and from 270 °C to 250 °C. Each change is introduced while keeping the other parameters constant at operating point.

The step sizes are chosen to keep the changes in the variables in the range of steady-state experiments. The results of dynamic experiments are given in Figures 5.5 to 5.7 for positive and negative step changes in screw speed, feed rate and temperature respectively.

It is observed from the Figures 5.5 to 5.7 that, the system responds differently for different inputs proving the highly non-linear structure of the process. In Figure 5.5.a response of the system to a positive deviation in screw speed is given while in Figure 5.5.b response in M_v to a negative deviation in SS is given. The natures of Figure 5.5.a and Figure 5.5.b are completely different. This trend is also seen in Figure 5.6 and 5.7. Accordingly, it is decided to use different process models depending upon the input deviations or simply depending upon the deviation in the output, M_v .

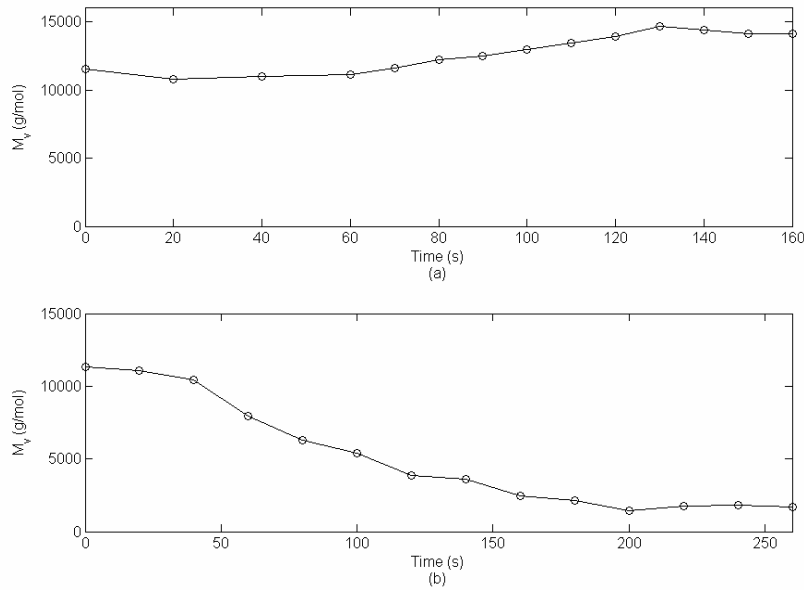


Figure 5.5: System responses to (a) positive (+25 rpm) and (b) negative (-50 rpm) steps on screw speed.

Figure 5.5 shows that screw speed or simply average residence time (ART) for the RPET in the extruder (see Table B.1) is more dominant on M_v than other mechanical effects in terms of degradation.

Considering Figure 5.6, as feed rate increases, amount of material in the extruder (filling ratio) increases, therefore heat and shear consumed per unit amount of material decreases, resulting in a increase in M_v of the product. Thus, as feed rate increases (Figure 5.6.a) M_v will increase (less degradation occurs), and as feed rate decreases (Figure 5.6.b) M_v will decrease (more degradation occurs).

In Figure 5.7 effect of temperature on M_v degradation is shown at constant screw speed and feed rate. The explanation of this trend cannot be done with the results of steady-state experiments and with the known literature, except that the formation of new bonds (branching/crosslinking) is lower (or does not exist at all) at 250 °C compared to 290 °C.

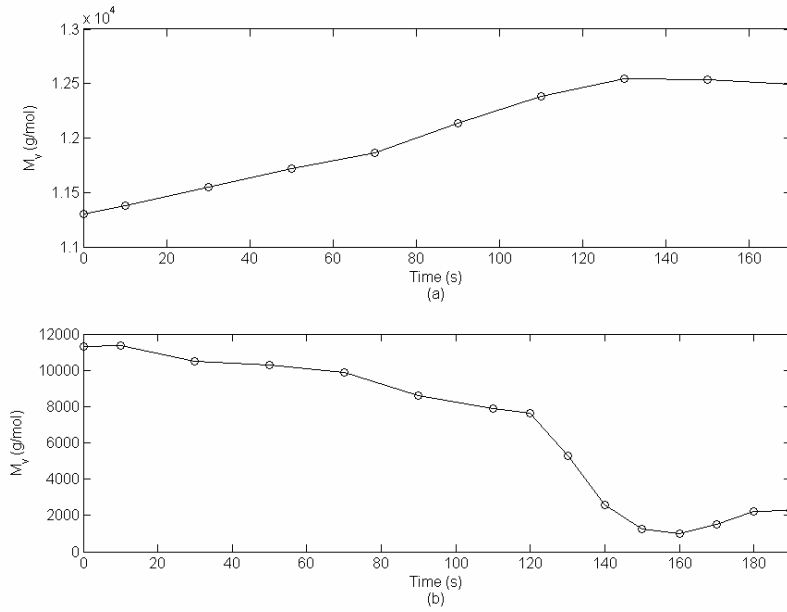


Figure 5.6: System responses to (a) positive (+1.04 g/min) (+25) and (b) negative (-1.42 g/min) (-25) steps on feed rate.

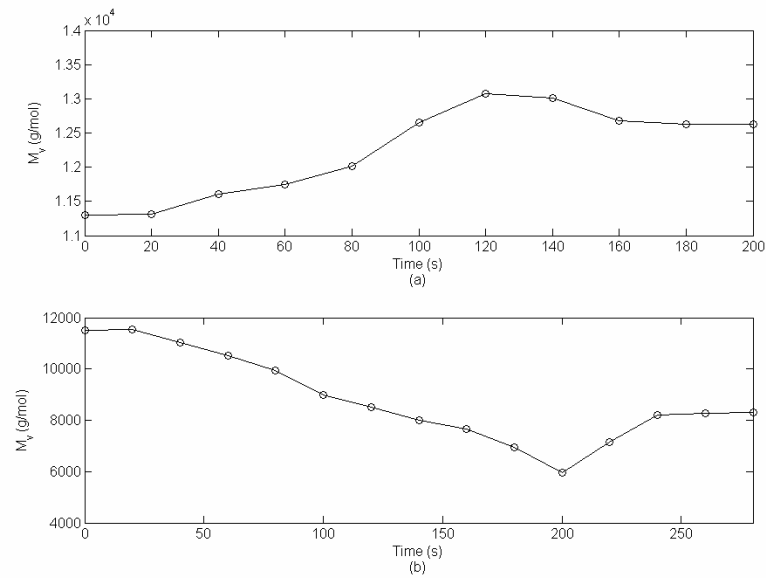


Figure 5.7: System responses to (a) positive (+20 °C) and (b) negative (-20 °C) steps on temperature.

5.4 Modeling Studies

As stated before, the experimental data obtained from the dynamic experiments are aimed to construct dynamic models of the process for control purposes. The experimental results which are illustrated in Figures 5.5 to 5.7 are revealed that the system behavior is highly nonlinear in nature. Therefore, the process needed to be modeled separately for the different changes in inputs as positive or negative. Thus, two separate models, one representing the response to positive and the other one to negative changes are obtained for screw speed, feed rate and temperature inputs separately and named as 'SS Model', 'FR Model' and 'T Model'. This model representation is shown in Figure 5.8.

As can be seen from the Figure 5.8, the input of each dynamic model is a different input variable of the extruder and the output of the model is the molecular weight of the product representing the dynamic behavior of the extruder machinery as a whole.

The experimental data must be represented analytically by a suitable model in order to be used in the control algorithm. Thus, in the modeling studies three different modeling techniques (single transfer functions, dual transfer functions and convolution models) are tried in order to obtain the best fit. In the first technique a transfer function is used for input-output relationship for the extrusion. In the second technique, two different transfer functions are used for two different consecutive periods throughout the transient response of the system. In the third technique, discrete convolution model is used. MATLAB software is utilized in all these studies.

In the modeling studies, experimental data are *normalized* with respect to initial steady state operating point. In normalization, each deviation variable (difference from the initial steady-state value) is divided by the magnitude of the step input. Consequently, it is assumed that the process is behaving linearly in the inputs' magnitude ranges. This assumption will be verified by the simulation studies done for different magnitudes of the inputs.

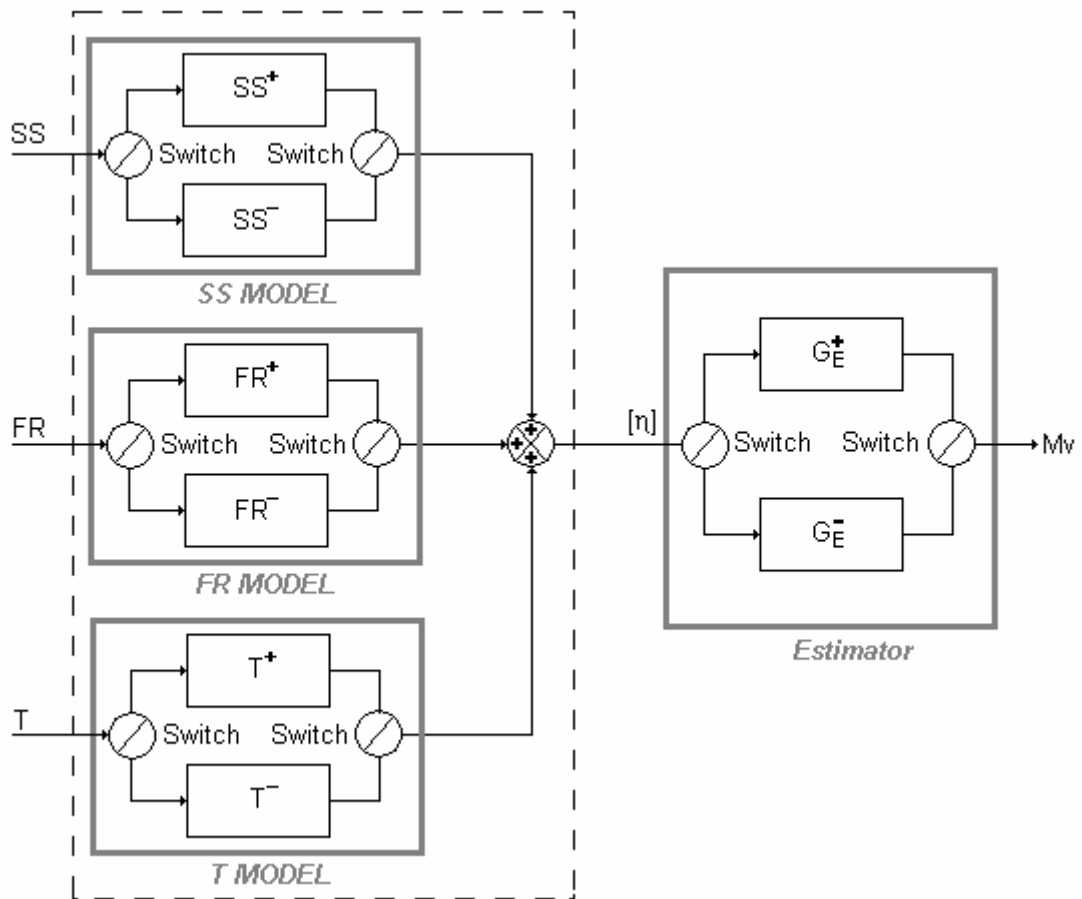


Figure 5.8: Model representation of the system.

The formulation of the normalization can be expressed as:

$$\Delta M_v^N = \frac{M_{vn} - M_{v0}}{\Delta m} \quad (5.1)$$

where ΔM_v^N is the *normalized molecular weight* of the product, m is the magnitude of the input (SS, FR or T) and n is the data points.

5.4.1 Modeling Technique 1: Single Transfer Functions

In this method, the process is tried to be modeled by a single transfer function. Different forms of transfer functions tested by changing the order (1st, 2nd and 3rd) and by changing the nature (integrator, dead-time and zero-poles).

'System identification toolbox' of MATLAB is used to identify the system automatically. However, toolbox failed in identification and custom codes (see Appendix D) are generated.

In modeling studies, for every parameter of the transfer function utilized a step response of the transfer function is obtained for a specific input and the absolute error, between it and the experimental data points are evaluated. The best fits giving the minimum integral absolute error (IAE) scores are given in Table 5.3 with their normalized IAE scores (divided by steady-state gains). The response curves to unit step changes are given in Figures 5.9 to 5.11 in terms of normalized molecular weight (ΔM_v^N) as a function of time.

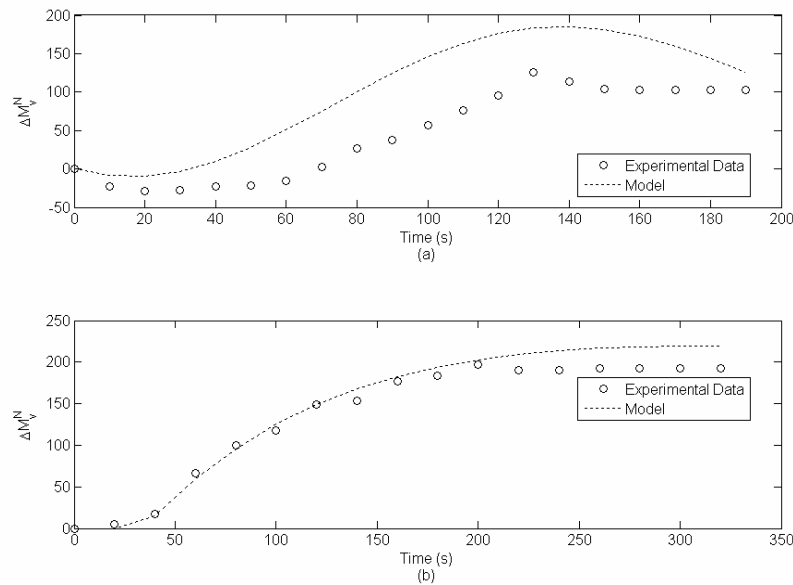


Figure 5.9: Plant and model responses to a (a) positive and (b) negative unit step changes in SS (single transfer function case).

Table 5.3: Single transfer function models and their normalized IAE scores.

Variable	Positive Model	Negative Model	IAE score of positive model	IAE score of negative model
Screw Speed (SS)	$\frac{-1832.66s + 102.4}{1.49s^3 + 1488.75s^2 + 7.41s + 1}$	$\frac{(4.79 \times 10^4 s + 192.1)e^{-33.9s}}{1.86 \times 10^4 s^2 + 252.69s + 1}$	10.73	1.09
Feed Rate (FR)	$\frac{9002.86s + 47.8}{3.18 \times 10^5 s^3 + 1.4 \times 10^4 s^2 + 205.72s + 1}$	$\frac{341.64}{7.42 \times 10^4 s^3 + 2074.24s^2 + 35.96s + 1}$	1.78	10.01
Temperature (T)	$\frac{66.4}{2260.91s^2 + 25.41s + 1}$	$\frac{1.48 \times 10^6 s + 160.4}{3.12 \times 10^7 s^3 + 3.81 \times 10^5 s^2 + 9298.85s + 1}$	2.18	2.26

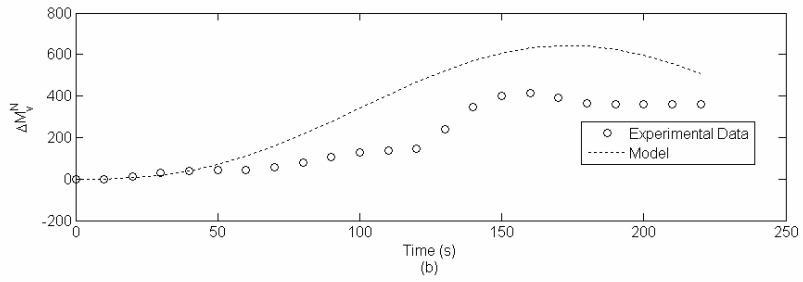
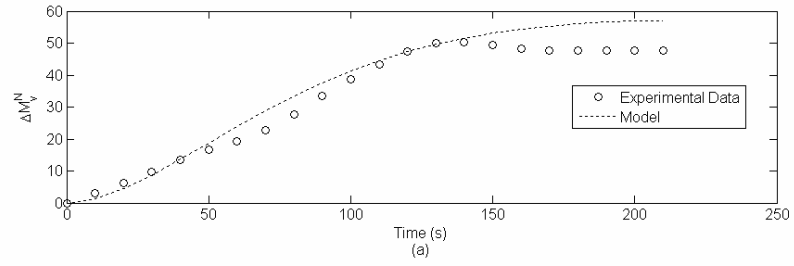


Figure 5.10: Plant and model responses to a (a) positive and (b) negative unit step changes in FR (single transfer function case).

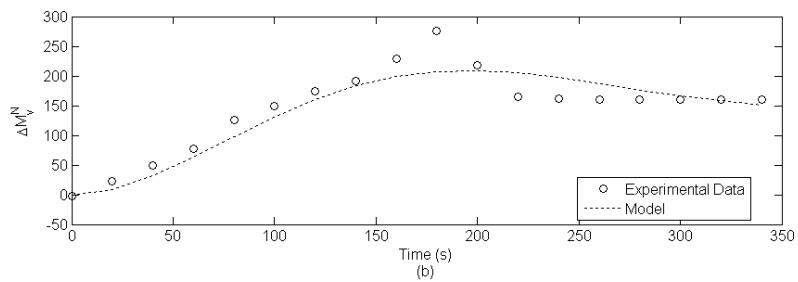
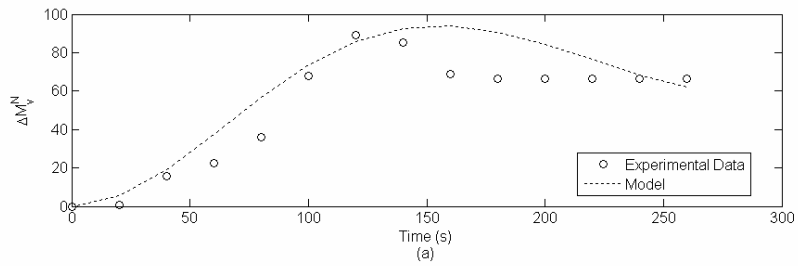


Figure 5.11: Plant and model responses to a (a) positive and (b) negative unit step changes in T (single transfer function case).

As can be seen from Figures 5.9 to 5.11 the system dynamics can be modeled by a single transfer function for each input. However the errors between the experimental data points and the models are large (large IAE scores) especially for the positive input in SS and negative input in FR.

5.4.2 Modeling Technique 2: Dual Transfer Functions

In the second method, two transfer functions are used to model the system. As stated before, the system under study is highly non-linear (Figures 5.5 to 5.7). Although transient positive and negative responses are considered differently, in modeling, also they can be modeled using different transfer functions for the whole time domain for a single input. Thus, for each of the six experimental data, two transfer functions can be used in such a way that, at the point where first transfer function loses the track of the experimental data, second one activates by deactivating the first one. Parameters of these transfer functions are adjusted by trial and error procedure as in the case of single transfer function modeling. In Figures 5.12 to 5.14 the response curves to unit step inputs are given using this 2nd modeling technique and in Table 5.4 the transfer function models, their acting time domains and normalized IAE scores (divided by steady-state gains) are given.

Table 5.4: Dual transfer function models and their normalized IAE scores.

Model	TF ₁	TF ₂	Switch Time	IAE Scores
SS ⁺	$\frac{-4593s + 102.4}{2486s^2 + 22s + 1}$	$\frac{458s + 7.12}{55s^2 + 11s + 1}$	120 th sec.	0.25
SS ⁻	$\frac{192.1}{2100s^2 + 76s + 1} e^{-9s}$	$\frac{6.4}{54s^2 + 5s + 1}$	200 th sec.	0.80
FR ⁺	$\frac{47.8}{3008s^2 + 48s + 1}$	$\frac{-2.12}{245s^2 + 24s + 1}$	130 th sec.	0.34
FR ⁻	$\frac{341.64}{5903s^2 + 168s + 1} e^{-5s}$	$\frac{-210.36}{79s^2 + 9s + 1}$	110 th sec.	0.38
T ⁺	$\frac{66.4}{2843s^2 + 2s + 1}$	$\frac{-23.55}{262s^2 + 251s + 1}$	120 th sec	0.39
T ⁻	$\frac{160.4}{4818s^2 + 28s + 1}$	$\frac{-2816s + 68.7}{287s^2 + 25s + 1}$	180 th sec.	0.45

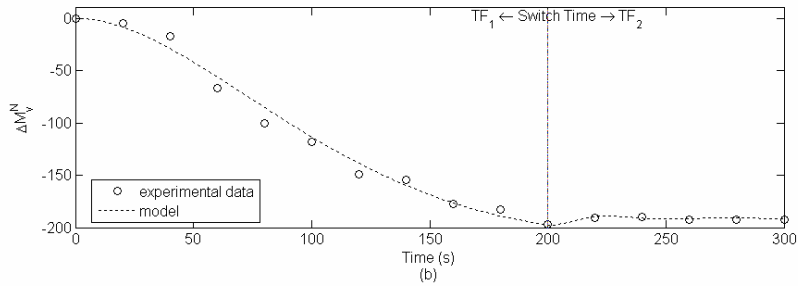
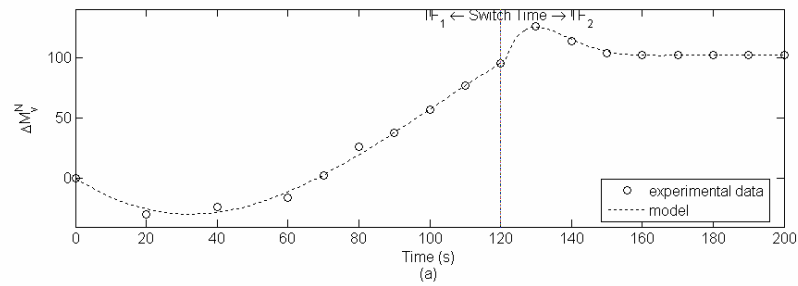


Figure 5.12: Plant and model responses to a (a) positive and (b) negative unit step changes in SS (dual transfer functions case).

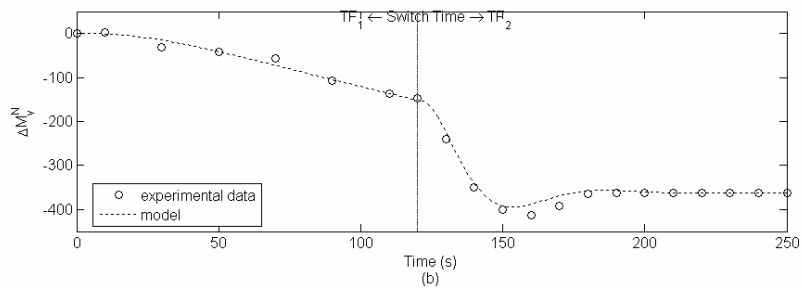
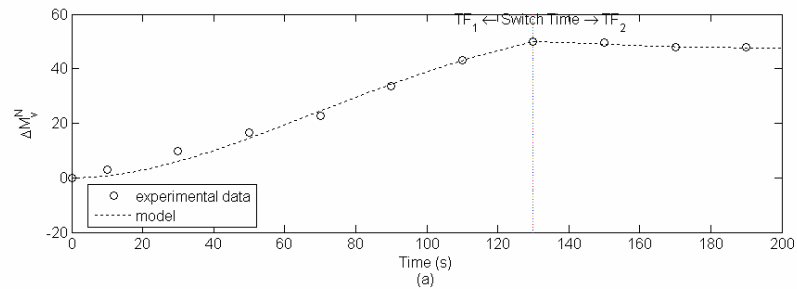


Figure 5.13: Plant and model responses to a (a) positive and (b) negative unit step changes in FR (dual transfer functions case).

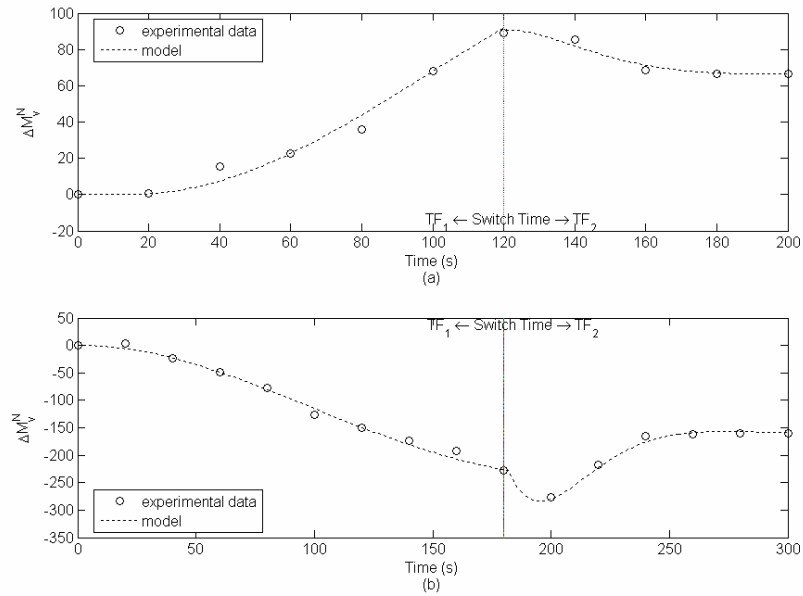


Figure 5.14: Plant and model responses to a (a) positive and (b) negative unit step changes in T (dual transfer functions case).

As can be seen from the Figures 5.12 to 5.14 and considering the IAE scores from Table 5.4, these models fit the experimental data much better than single transfer functions. However, during the control operation, manipulated variable (SS) changes and the controlled variable (M_v) is tried to be kept constant or to track the set point. In these manipulations the model based controller has to be switched on different models (positive/negative/TF₁/TF₂). This cannot be solved by a single algorithm. Therefore, this modeling technique is not considered to be user friendly.

5.4.3 Modeling Technique 3: Discrete Convolution Models

It is well known that in the model predictive control, MPC, algorithm discrete convolution models are widely and effectively used. In the convolution model, the output is evaluated by using the experimentally obtained step response coefficients (see Figure 3.4) and the past values of the manipulated variables. The model equation is given in Equation 5.2 [Seborg et al., 1989]. Thus, the model is considered to represent linearly the responses to all different inputs in the range studied.

$$\Delta y_{n+1} = \sum_{i=1}^n a_n \Delta m_{n+1-i} \quad (5.2)$$

where Δy is the output in deviation form, a is the step response coefficient and Δm is the manipulated variable (model input) in deviation form.

In this study the experimentally obtained step response data can be curve fitted as 'shape preserving function' using 'curve fit toolbox' of MATLAB and step response coefficients (a_n) are obtained as a function of time. Comparison of model and actual system outputs are given in Figures 5.15 to 5.17.

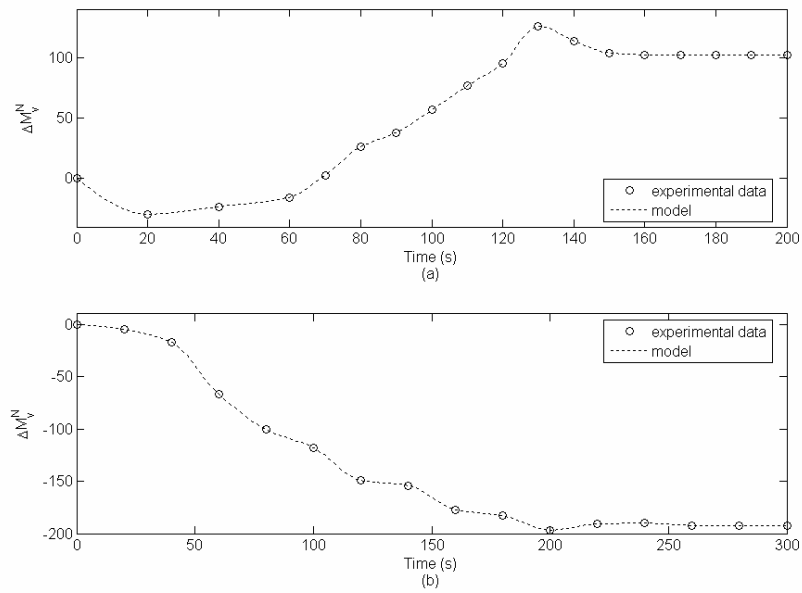


Figure 5.15: Plant and model responses to a (a) positive and (b) negative unit step changes in SS (discrete convolution models case).

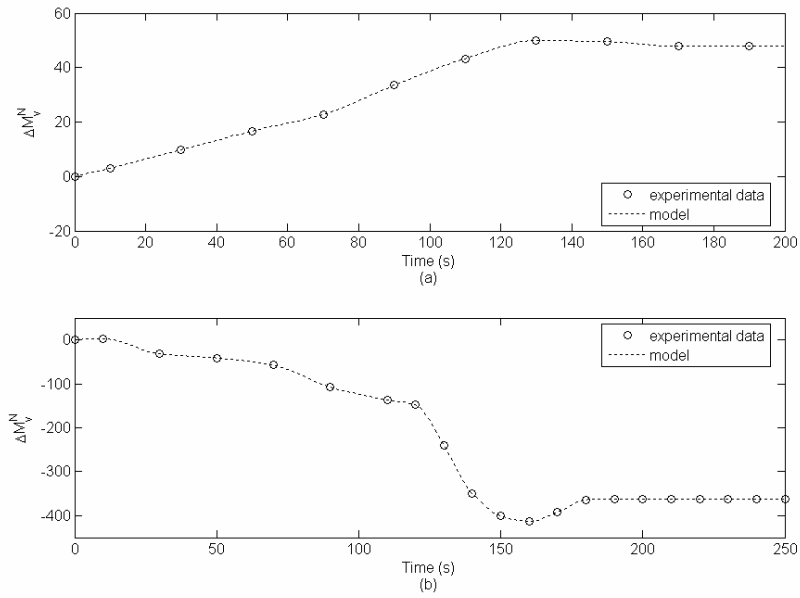


Figure 5.16: Plant and model responses to a (a) positive and (b) negative unit step changes in FR (discrete convolution models case).

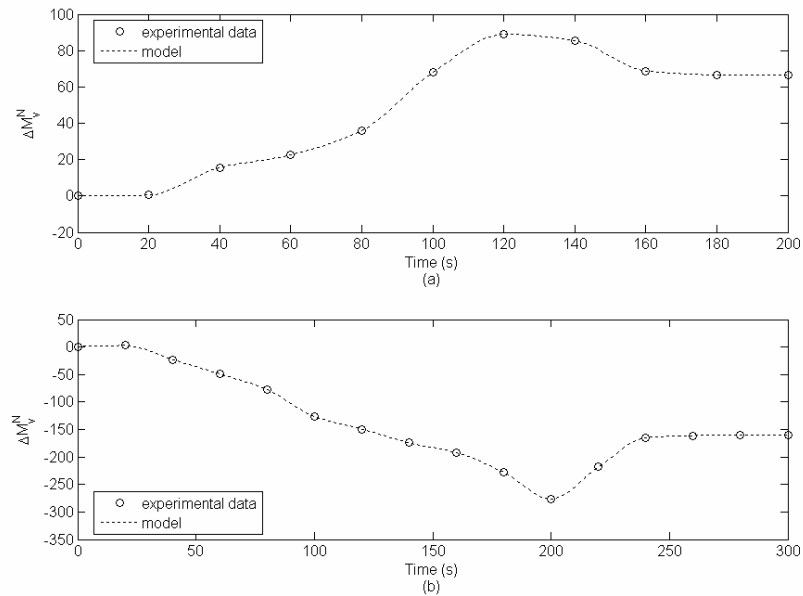


Figure 5.17: Plant and model responses to a (a) positive and (b) negative unit step changes in T (discrete convolution models case).

In Figures 5.15 to 5.17, the digital model outputs (in 1 second intervals) are shown in comparison to experimental data given in 10 seconds intervals. The disadvantage using this method is that, they are not compatible with MATLAB, i.e. there does not exist a pre-constructed library, function or toolbox for the discrete convolution models. Thus, codes working in continuous time have to be written for this case (see Appendix D).

5.5 Control Studies

After the dynamic behavior of the plant is modeled, the final step is to design a proper controller in a control loop. In the design of the control loop, the first step is the choice of manipulated variable(s) for the control of system output. After deciding on manipulated and controlled variable pair, a control scheme is designed and on this scheme, MPC and PID controllers are tested and compared. The system under study (Figure 5.8) is a multi input single output (MISO) system. The inputs are SS, FR and T, and the output is the product property. The output, which is the product property, is determined in terms of molecular weight (M_v) and this is measured by intrinsic viscosity ($[\eta]$).

5.5.1 Singular Value Decomposition

The design of a control system, when there are more than one input, necessitates the use of the singular value decomposition, SVD, technique for the selection of the manipulated – controlled variable pairs. By this method, it is possible to find out which output is most sensitive to which input. SVD analysis calculations for the system under study are given below.

As stated before, the system is highly non-linear and can only be represented by different models (positive and negative) for different inputs (as positive and negative).

The steady-state M_v can be expressed in terms of input variables for positive and negative models as given in Equations 5.3.a and 5.3.b respectively.

$$M_v^+ = \begin{bmatrix} K_{SS}^+ & K_{FR}^+ & K_T^+ \end{bmatrix} \begin{bmatrix} SS^+ \\ FR^+ \\ T^+ \end{bmatrix} \quad (5.3.a)$$

$$M_v^- = \begin{bmatrix} K_{SS}^- & K_{FR}^- & K_T^- \end{bmatrix} \begin{bmatrix} SS^- \\ FR^- \\ T^- \end{bmatrix} \quad (5.3.b)$$

where K^+ and K^- symbols denote the steady state gains for the corresponding inputs, and superscripts '+' and '-' denotes the relevant model parts. Replacing steady state gain values in Equations 5.3.a and 5.3.b gives:

$$M_v^+ = \begin{bmatrix} 102.4 & 47.8 & 66.4 \end{bmatrix} \begin{bmatrix} SS^+ \\ FR^+ \\ T^+ \end{bmatrix} \quad (5.4.a)$$

$$M_v^- = \begin{bmatrix} 192.1 & 361.6 & 160.4 \end{bmatrix} \begin{bmatrix} SS^- \\ FR^- \\ T^- \end{bmatrix} \quad (5.4.b)$$

Decomposing steady state gain matrices (\mathbf{K}^+ and \mathbf{K}^-) in Equation 5.4.a and 5.4.b gives:

$$\mathbf{K}^+ = \begin{bmatrix} 1 \end{bmatrix} \begin{bmatrix} 131.0708 & 0 & 0 \end{bmatrix} \begin{bmatrix} 0.7813 & -0.5066 & -0.3647 \\ 0.5066 & 0.8559 & -0.1037 \\ 0.3647 & -0.1037 & 0.9253 \end{bmatrix} \quad (5.5.a)$$

$$\mathbf{K}^- = \begin{bmatrix} 1 \end{bmatrix} \begin{bmatrix} 439.7887 & 0 & 0 \end{bmatrix} \begin{bmatrix} 0.4368 & -0.3647 & -0.8223 \\ 0.3647 & 0.9074 & -0.2087 \\ 0.8223 & -0.2087 & 0.5294 \end{bmatrix} \quad (5.5.b)$$

SVD¹ shows that the best pair is screw speed – molecular weight for positive model and temperature – molecular weight for negative model, considering the largest elements in the first columns of \mathbf{V}^T matrices in the Equations 5.5.a and 5.5.b.

However, in control it is not possible to change the manipulated variable when the input changes. Thus, beside SVD recommendation, choice of the variables must also be based on expert knowledge of the process. Among the inputs, manipulating the screw speed is the fastest and the easiest. The extruder responds to the changes in the screw speed setting

¹ Second and the third column of the \mathbf{V}^T matrices should be omitted as they correspond to the zero elements of the singular value vector (Σ).

almost instantaneously. On the other hand, the changes in the temperature are responded much more slowly. Furthermore, in an actual plant, the feed flow rate is kept constant for the sake of the operations following the extrusion. For these reasons, screw speed is chosen as the manipulated variable, while temperature and feed rate are considered to be disturbances.

The choice of the disturbances is based on the facts that a blockage or disorder in the feed flow is always possible. Also, there can be failures in the heaters or changes in cooling water, resulting in unwanted changes in the barrel temperature.

It should be noted that no measurement of input FR is available in the process other than the adjustment of the extruder. But having the model, disturbances on the feed flow is also tested as if measurements are available.

5.5.2 Design of Control Scheme

As stated before, the objective of the control system is to control the molecular weight (M_v) of the product leaving the extruder under the effect of disturbances or in the case of set point changes. However, as in this study, online measurement of the desired property (M_v) may not be possible. Thus, a modified inferential control scheme can be used, in which an *estimator* estimates the desired property by using the secondary online measurements available from the plant and supplies necessary feedback data. The product quality can be determined by on-line viscosity measurements which can give the M_v of the product. Thus, a feedback control loop is designed as shown in Figure 5.18. In this scheme among the input variables such as SS, FR and T; SS is chosen as the manipulated variable (see Chapter 5.5.1) while FR and T are chosen as probable disturbances. Other disturbances to the system may be the PET composition. This, of course, can be measured from the batch introduced and this information can be used for first settings of the operation for a required product quality. As it is found experimentally that the system is highly non-linear, the controllers are made of two compartments, G_c^+ and G_c^- . G_c^+ is using of the 'positive' process model and the other, G_c^- , is using of the 'negative' process model. A 'switch' in the entrance of the controller decides which model to run, basing on the deviation of M_v from its initial desired value.

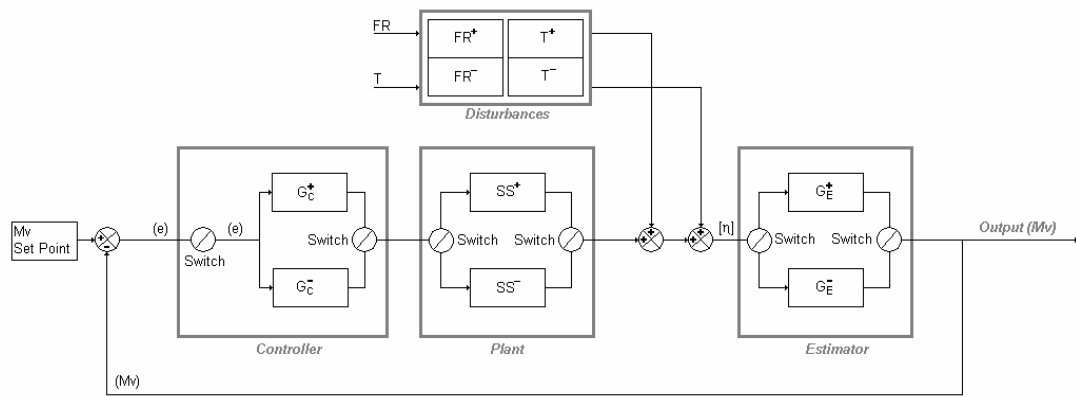


Figure 5.18: Designed control system.

Also, both in the disturbance models G_p^+ and G_p^- , and in the estimator G_E^+ and G_E^- exist.

5.5.3 PID Control

PID controllers are used in the designed control system. PID controllers are designed using the convolution models of the system by utilizing 'continuous cycling' or 'Ziegler-Nichols' method with 'modified Z-N settings'. PID parameters are calculated by using the relationships given in the literature [Seborg et al., 1989] (see Appendix E), and the results are given in Table 5.5. In Figure 5.19 responses of set point tracking for the PID controllers are given. The set points are the 10% of the model gains. The normalized IAE scores for positive and negative models are given in Table 5.5. IAE scores are normalized with respect to steady-state gains and time ranges.

Table 5.5: PID settings utilizing modified Z-N method (Some Overshoot) [Seborg et al., 1989], and normalized IAE scores of set point tracking (Figure 5.19).

	K_c	τ_i	τ_D	IAE Score
PID ⁺	0.0025	2.7399×10^5	0.1513	4.85
PID ⁻	0.0058	1.0357×10^4	0.2165	0.01

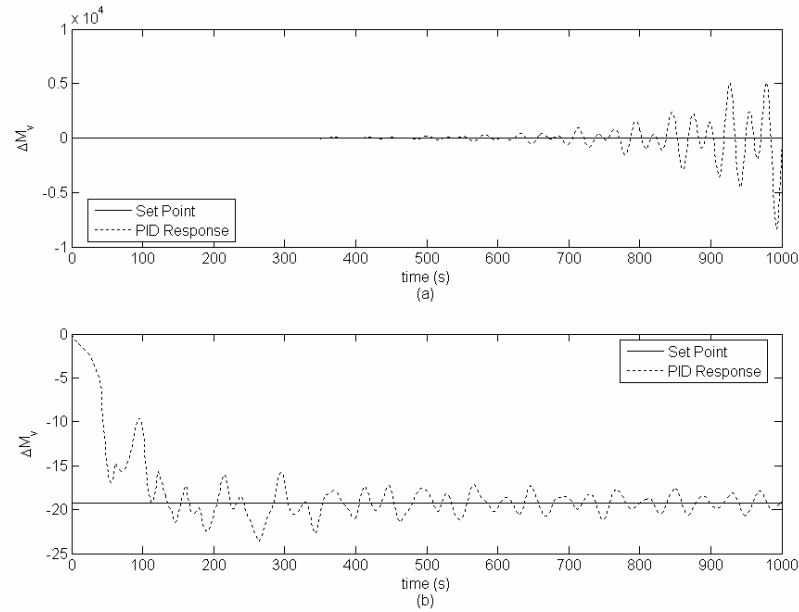


Figure 5.19: Set point tracking of PID controllers of (a) positive and (b) negative models, tuned using modified Z-N settings (Some Overshoot) [Seborg et al., 1989].

As can be seen from the Figure 5.19 the system shows an unstable performance for both positive and negative inputs and settling times are very large for these settings. Therefore, the controllers are further fine tuned by trial – error procedure. The fine tuned PID settings are given in Table 5.6.

Table 5.6: Fine tuned PID settings for PID⁺ and PID⁻.

	K_c	τ_i	τ_D
PID ⁺	2.50×10^{-3}	6.85×10^{-5}	3.03×10^{-2}
PID ⁻	3.50×10^{-3}	6.21×10^{-5}	2.60×10^{-2}

These PID settings are very small and cannot be implemented on a nominal operating industrial plant controller. However, if a computer is used for the PID controller, then these settings can be implemented. Therefore, in this study, for comparison with the MPC, which can only be implemented via computers, the PID settings as given in Table 5.6 are used. Furthermore, constraints are also placed on PID outputs (SS) to be able to compare PID

controller with the MPC. The lower limit implemented on PID^+ is 0 rpm and the upper and lower limits for PID^- are 0 rpm and -50 rpm respectively.

In order to observe the set point tracking response of the controller, step changes listed in Table 5.7 are introduced. For the disturbance studies, the disturbances are introduced as ± 25 in FR (corresponding to +1.04 g/gmol and -1.42 g/gmol), and ± 10 °C in T.

Table 5.7: The magnitudes and the time of changes of the given set point changes.

Time (s)	0	1000	2000	3000	4000	5000
Magnitude (g/mol)	+1200 (+10.4%)	-550 (-4.8%)	-650 (-5.7%)	-9050 (-78.7%)	+7450 (+64.8%)	+1600 (+13.9%)

Control loop is built using 'SIMULINK toolbox' of MATLAB for the PID controller (see Appendix D). PID performances are tested for set point tracking and disturbance rejection cases. The results are given in Figures 5.21 to 5.29.

5.5.4 Model Predictive Control (MPC)

In the design and testing of MPC, as for PID controllers, two parallel working SISO MPCs are constructed using the 'model predictive control toolbox' of MATLAB, for *non-linear constrained MPC*.

5.5.4.1 Process Models for MPC

In order to generate a step response process model that can be used in MPC algorithm, ARX models are formulated and used to obtain the molecular weight response to a step change in screw speed. This is shown in Figure 5.20 for the positive and the negative inputs. As can be seen from the Figures 5.5 to 5.7, the system is highly non-linear and the response behavior is very different for input values of positive and negative (Figure 5.20.a and 5.20.b).

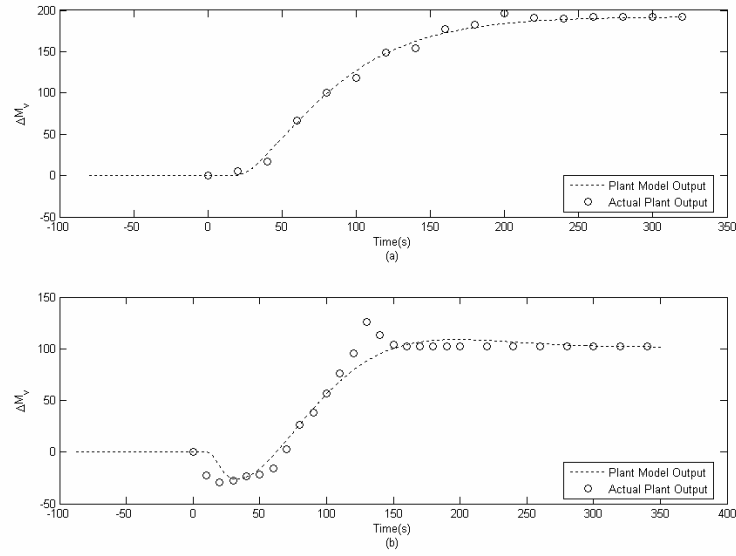


Figure 5.20: Responses of ARX models to (a) positive and (b) negative unit step changes in SS.

5.5.4.2 MPC Tuning

Tuning of predictive controllers are carried out by trial and error procedure, basing on the recommendations in the literature [Seborg et al., 1989]. MPC tuning parameters are given in Table 5.8.

In the preliminary control studies it is seen that MPC fails to reject the disturbances. This problem was also seen in a previous study [Obut, 2005]. MPC algorithm assumes that the disturbances have a 'constant-linear' nature. However, in this work, the trends of disturbances resemble the response of a first order transfer function to a step input. Thus, designed MPCs usually fail to handle these disturbances. This problem is solved by changing the disturbance estimation type from constant to 'step' in G_c^+ and to 'ramp' in G_c^- .

Table 5.8: MPC tuning parameters.

Parameter	MPC ⁺	MPC ⁻
Prediction Horizon	200	100
Control Horizon	1	1
Output weights / Input weights	1	1
Disturbance Type And Magnitude	Step (20)	Ramp (10)
Constraints On Manipulated Variables	Min: 0 Max: ∞	Min:-50 Max:0

Designed MPCs are tested for set point tracking (see Table 5.7) and disturbance rejection performances. In Figure 5.21 the MPC responses for set point tracking is given together with PID performances for comparison.

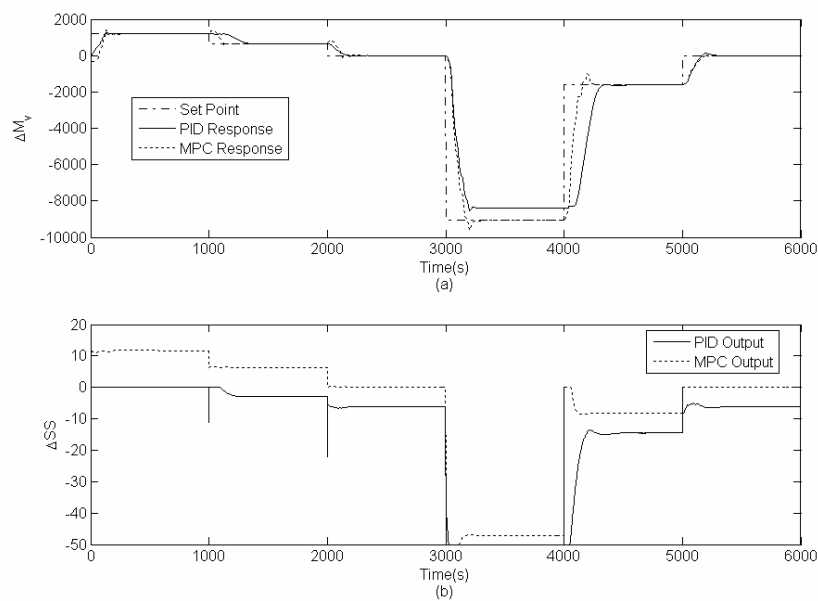


Figure 5.21: Set point tracking responses of PID and MPC.

Normalized IAE scores calculated from Figure 5.21 are given in Table 5.9. In normalization of IAE scores, calculated IAE score is divided by the input magnitude and by the time range in which it is calculated.

Table 5.9: Normalized IAE scores of controllers throughout set point tracking.

Time range (s)	0 to 1000	1000 to 2000	2000 to 3000	3000 to 4000	4000 to 5000	5000 to 6000
PID	1.00	1.19	0.01	0.99	0.21	0.00
MPC	0.99	1.17	0.01	0.99	0.21	0.00

The performances of the controllers for tracking the set point for the given step sizes are very good and very similar to each other. Although in Figure 5.21 the deviations for larger step sizes ($3000 < t < 4000$) are larger, this cannot be reflected in normalized IAE scores, which is done in order to be able to compare IAE scores for different step sizes.

In Figures 5.22 and 5.23, the controller responses in terms of deviation in molecular weight, ΔM_v , are given for disturbance rejection for 100% of positive and negative FR changes used in experiments respectively.

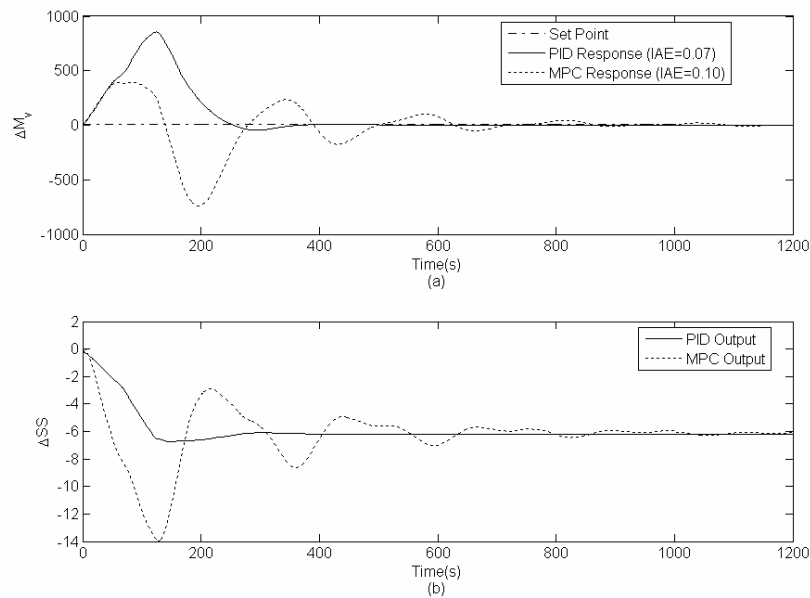


Figure 5.22: Disturbance rejection responses of PID and MPC (+25 or +1.04 g/gmol step disturbance on FR).

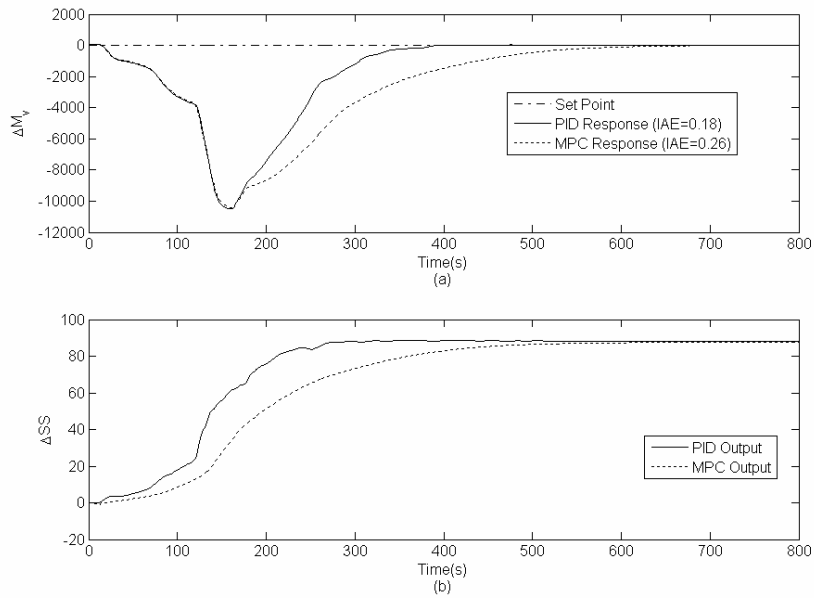


Figure 5.23: Disturbance rejection responses of PID and MPC (-25 or -1.42 g/gmol step disturbance on FR).

It is seen from Figures 5.22 and 5.23 that IAE scores are 0.07 and 0.10 for positive input in FR and 0.18 and 0.26 for negative input in FR, for PID and MPC respectively. Besides its lower IAE scores, the settling times of the PID controllers are also smaller compared to MPC.

Disturbance rejection performances of the controllers for positive and negative disturbances in temperature are given in Figures 5.24 and 5.25. The disturbance magnitudes studied are the 50% of the T changes used in the experiments.

Figures 5.24 and 5.24 show that the controllers' responses are similar to the cases where disturbances are introduced to FR (Figures 5.22 and 5.23). The IAE scores of the controllers are 0.08 and 0.16 for positive disturbance in T, and 0.21 and 0.22 for negative disturbance in T, for PID and MPC respectively. The reason of larger settling times and IAE scores seem to be the slower response of the extruder to the changes in temperature.

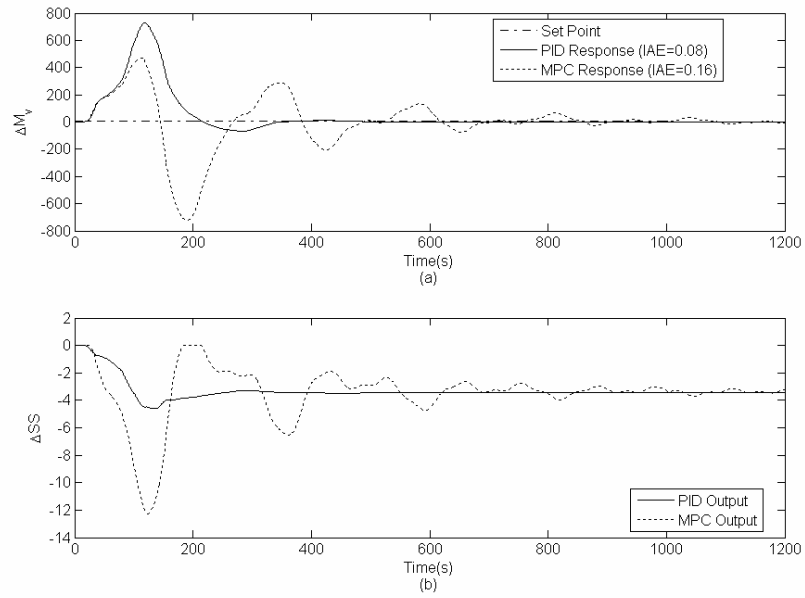


Figure 5.24: Disturbance rejection responses of PID and MPC (+10 °C step disturbance on T).

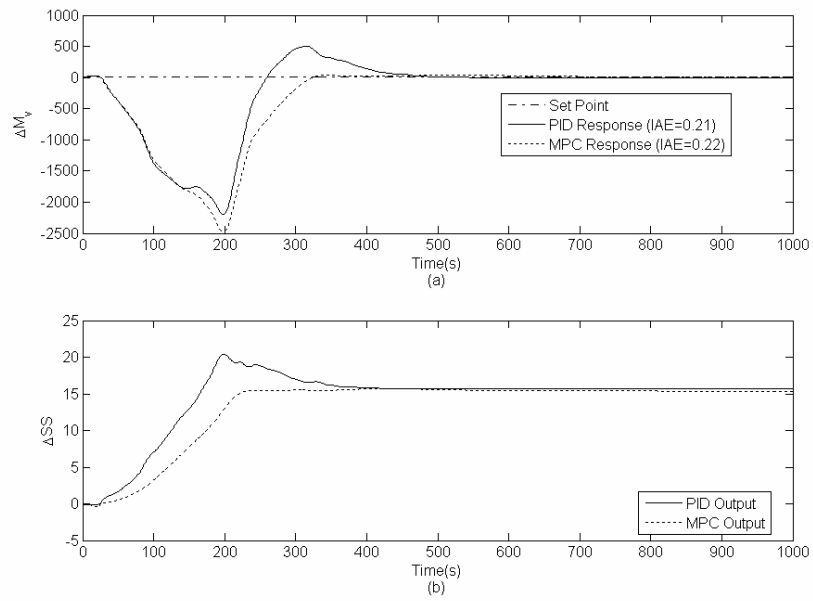


Figure 5.25: Disturbance rejection responses of PID and MPC (-10 °C step disturbance on T).

IAE scores and settling times calculated from Figures 5.24 and 5.25 are given in Table 5.10. From Figures 5.22 to 5.25 and Table 5.10 it can be seen that both controllers are successful in eliminating the effects of the disturbances, PID being a little better.

Table 5.10: Normalized IAE scores and settling times of controllers in disturbance rejection performances.

Case	MPC		PID	
	IAE Score	Settling Time	IAE Score	Settling Time
Positive Disturbance on FR	0.10	1200	0.07	1000
Negative Disturbance on FR	0.26	700	0.18	550
Positive Disturbance on T	0.16	1200	0.08	1000
Negative Disturbance on T	0.22	900	0.21	500

The performances of the controllers for different step changes in the disturbances (50% of the experimentally studied range in FR and 100% in T) are also investigated and the responses are given in Figures 5.26 to 5.29.

When Figures 5.22 to 5.25 are compared to Figures 5.26 to 5.29, it can be seen that the responses of the controllers, PID and MPC, changes linearly with the magnitude of the disturbance. This conclusion can also be observed from the IAE scores given in Tables 5.10 and 5.11. These results are also in agreement with the assumption that the plant would behave linearly in the studied ranges of the inputs. However, the settling times of the controllers are not affected much by the magnitude of the disturbance (Tables 5.10 and 5.11).

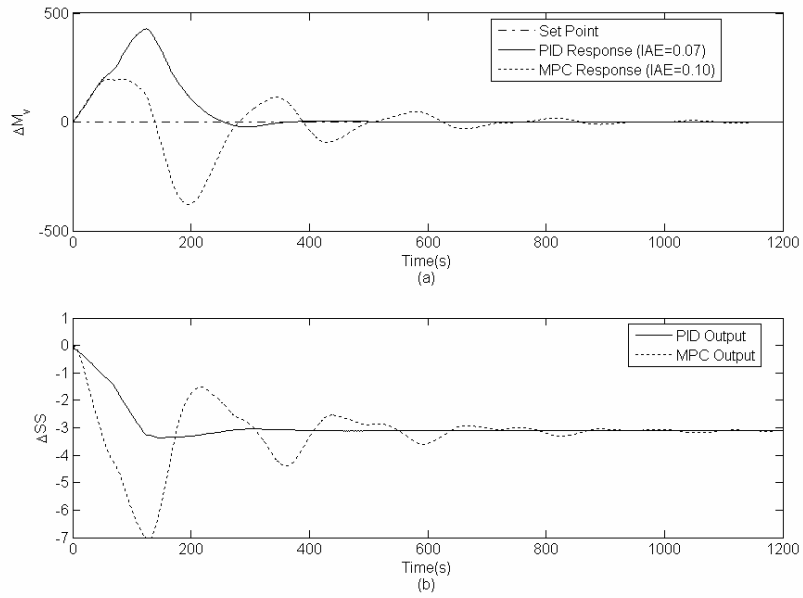


Figure 5.26: Disturbance rejection responses of PID and MPC (+12.5 or +0.57 g/gmol step disturbance on FR).

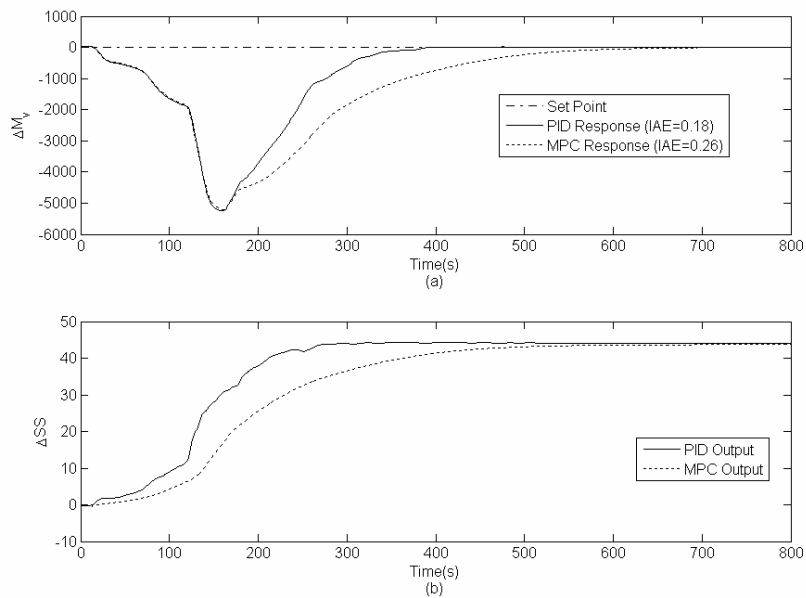


Figure 5.27: Disturbance rejection responses of PID and MPC (-12.5 or -0.71 g/gmol step disturbance on FR).

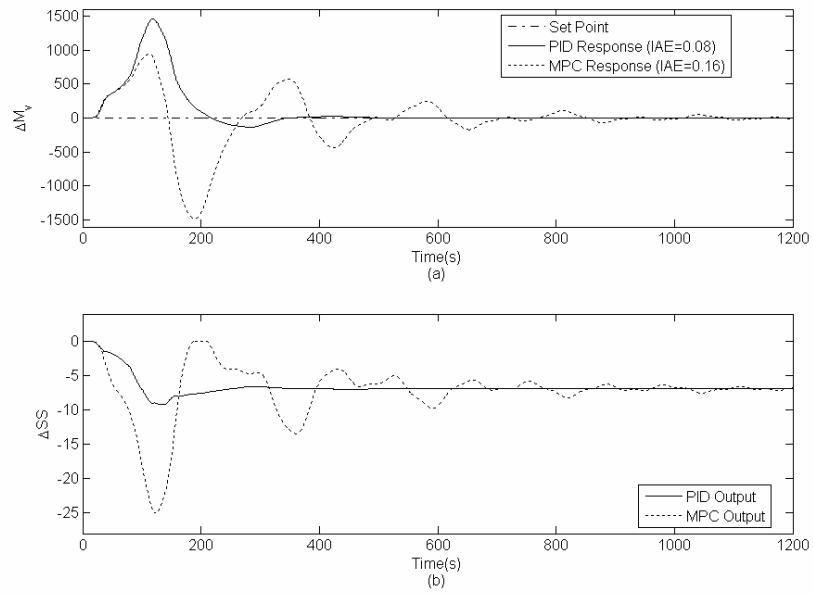


Figure 5.28: Disturbance rejection responses of PID and MPC (+20 °C step disturbance on T).

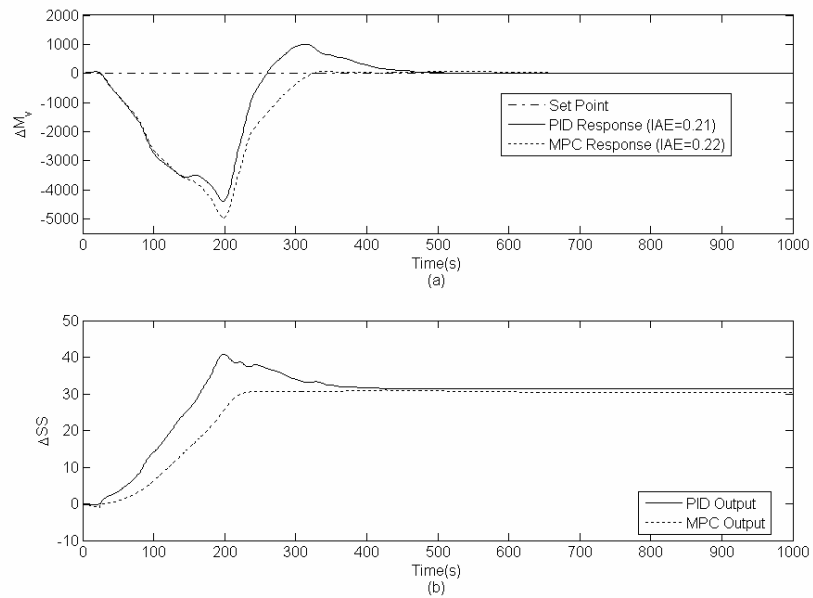


Figure 5.29: Disturbance rejection responses of PID and MPC (-20 °C step disturbance on T).

5.5.5 Robustness Analysis

The robustness analysis is carried out to observe the performance of the controllers under modeling errors. In order to change the plant behavior, the gains of the plant models are changed by +10%.

Figures 5.30 and 5.31 show the controllers' set point tracking performances for the 10% increase and 10% decrease in model gains respectively. Normalized IAE scores calculated from these figures are given in Tables 5.12 and 5.13. The IAE scores are normalized by dividing with the magnitude of the change and corresponding time range.

It is observed from Figure 5.30 that MPC cannot achieve the set point due to the constraints on manipulated variable for a relatively large negative set point value (-9050 g/mol). However, PID achieves the set point by applying more control actions. Figure 5.31 shows the case where the plant model gains are reduced by 10%. In this case, for the same set point value, both controllers fail to achieve the set point although PID gives less offset by keeping the screw speed on its lower limit.

In set point tracking, the controllers show similar responses in the case of modeling errors (Figures 5.30 and 5.31) compared to the case without modeling error (Figure 5.21), producing almost the same IAE scores (Tables 5.9, 5.11 and 5.12).

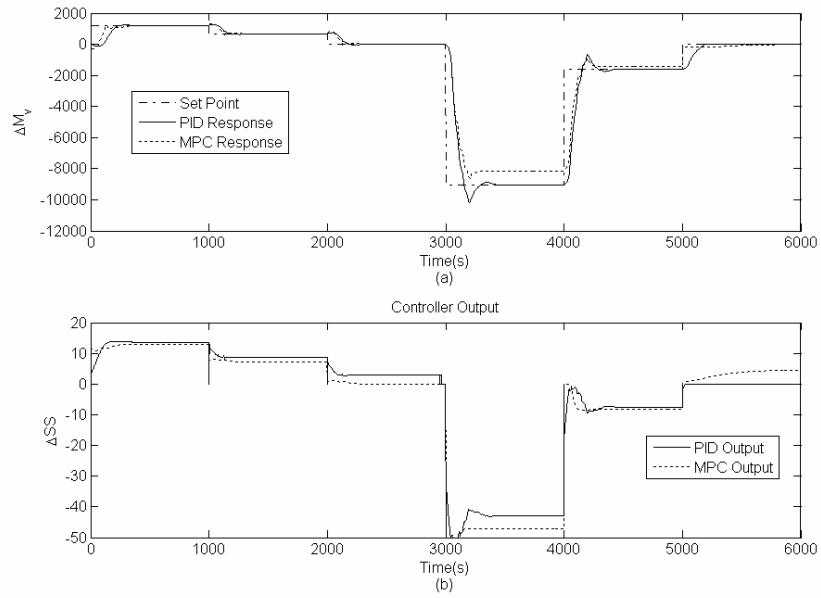


Figure 5.30: Set point tracking responses of PID and MPC (10% increase in model gains).

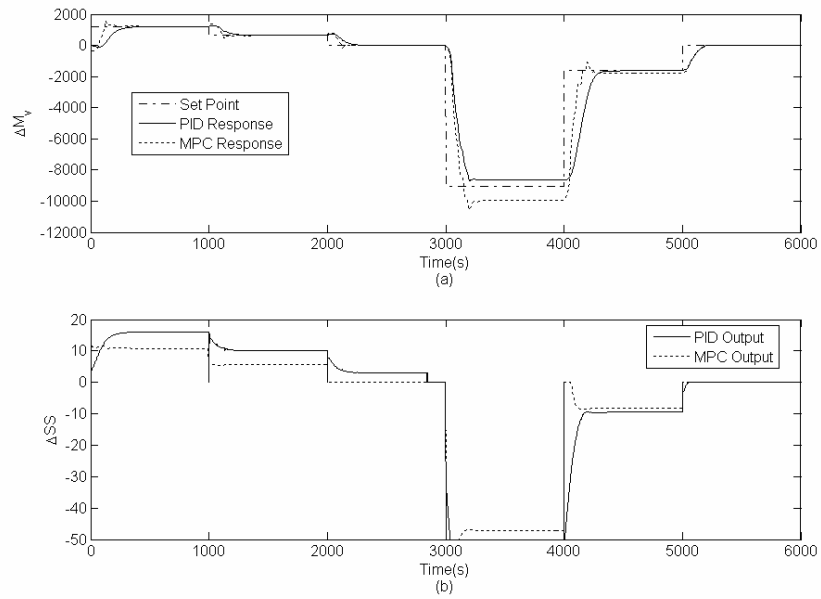


Figure 5.31: Set point tracking responses of PID and MPC (10% decrease in model gains).

Table 5.11: Normalized IAE scores of controllers throughout set point tracking (10% increase in model gains).

Time range (s)	0 to 1000	1000 to 2000	2000 to 3000	3000 to 4000	4000 to 5000	5000 to 6000
PID	0.99	1.16	0.00	0.99	0.21	0.00
MPC	0.99	1.17	0.01	0.99	0.21	0.00

Table 5.12: Normalized IAE scores of controllers throughout set point tracking (10% decrease in model gains).

Time range (s)	0 to 1000	1000 to 2000	2000 to 3000	3000 to 4000	4000 to 5000	5000 to 6000
PID	0.99	1.17	0.00	1.00	0.21	0.00
MPC	0.99	1.17	0.01	0.99	0.21	0.00

Figures 5.32 and 5.33 show the controllers' responses to the disturbances in feed rate for the case where the model gains are increased by 10%. Similarly, Figures 5.34 and 5.35 show the responses to the disturbances in feed rate where the model gains are decreased by 10%. The IAE scores calculated from these figures are given in Tables 5.13 and 5.14.

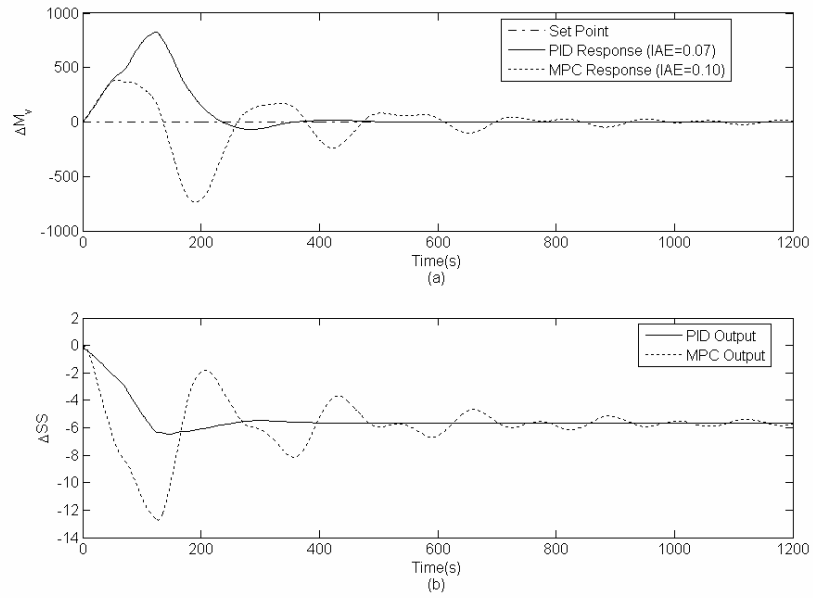


Figure 5.32: Disturbance rejection responses of PID and MPC (+1.04 g/gmol step disturbance on FR) (10% increase in model gains).

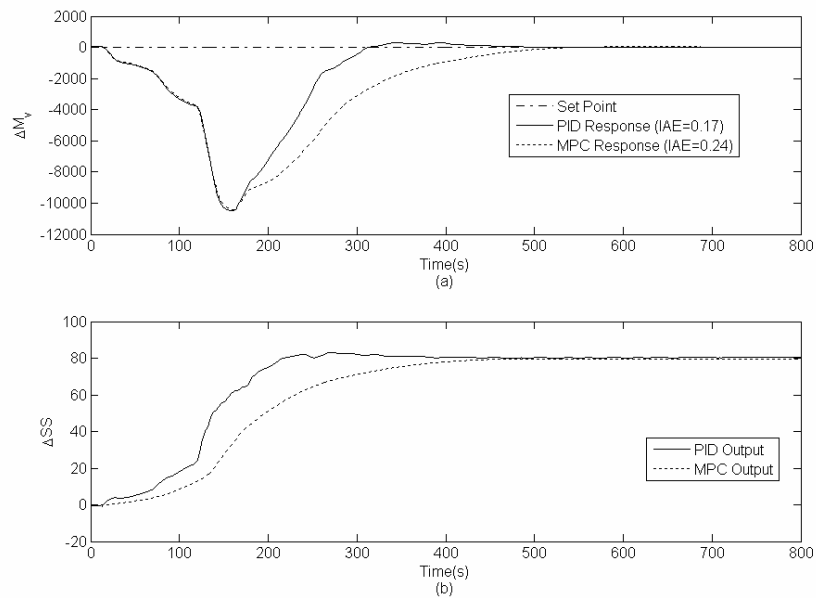


Figure 5.33: Disturbance rejection responses of PID and MPC (-1.42 g/gmol step disturbance on FR) (10% increase in model gains).

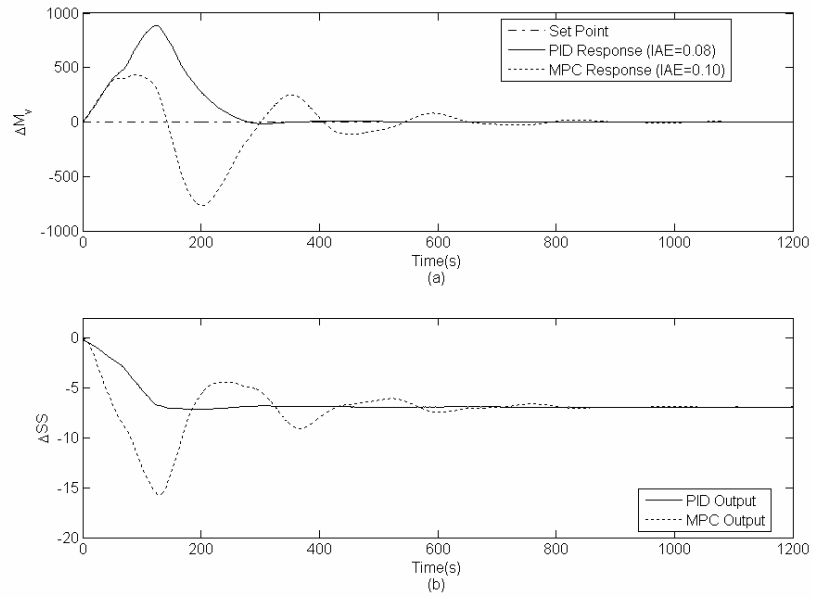


Figure 5.34: Disturbance rejection responses of PID and MPC (+1.04 g/gmol step disturbance on FR) (10% decrease in model gains).

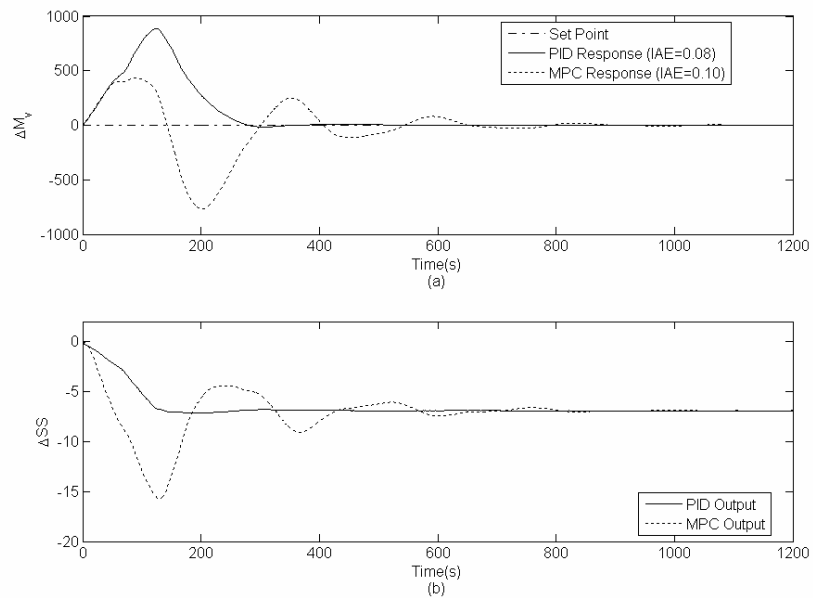


Figure 5.35: Disturbance rejection responses of PID and MPC (-1.42 g/gmol step disturbance on FR) (10% decrease in model gains).

Figures 5.36 and 5.37 show the controllers' responses to the disturbances in temperature for the case where the model gains are increased by 10%. Similarly, Figures 5.38 and 5.39 show the responses to the disturbances in temperature where the model gains are decreased by 10%. The IAE scores calculated from these figures are given in Tables 5.13 and 5.14.

It can be seen from Figures 5.32 to 5.35 that the modeling errors do not have strong effect on the disturbance rejection behaviors of the controllers. Although there are small differences in IAE scores, PID and MPC respond to the disturbances similarly compared to the case which there is no modeling error (Figures 5.22 to 5.25).

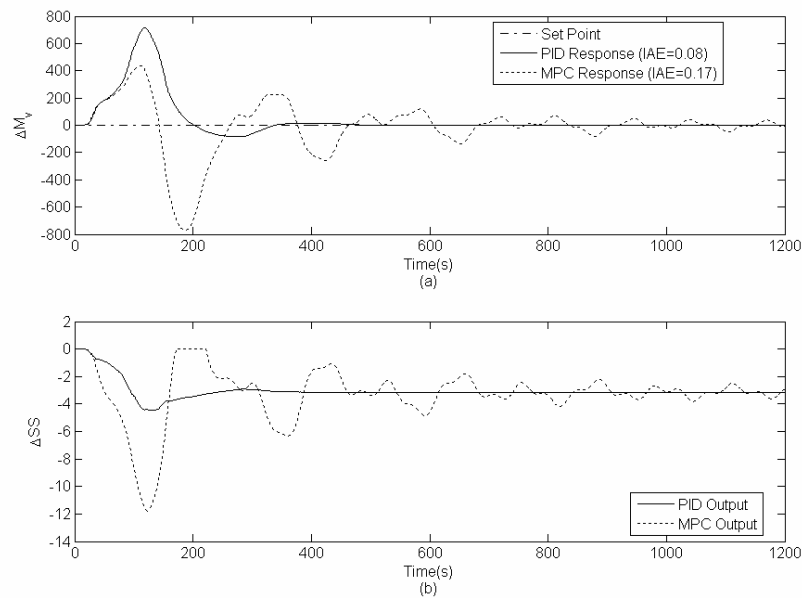


Figure 5.36: Disturbance rejection responses of PID and MPC (+10 °C step disturbance on T) (10% increase in model gains).

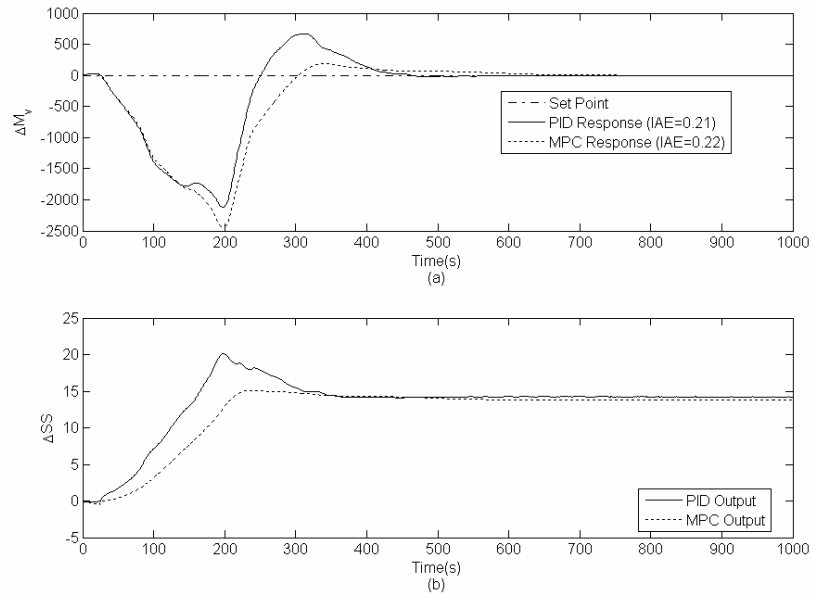


Figure 5.37: Disturbance rejection responses of PID and MPC (-10 °C step disturbance on T) (10% increase in model gains).

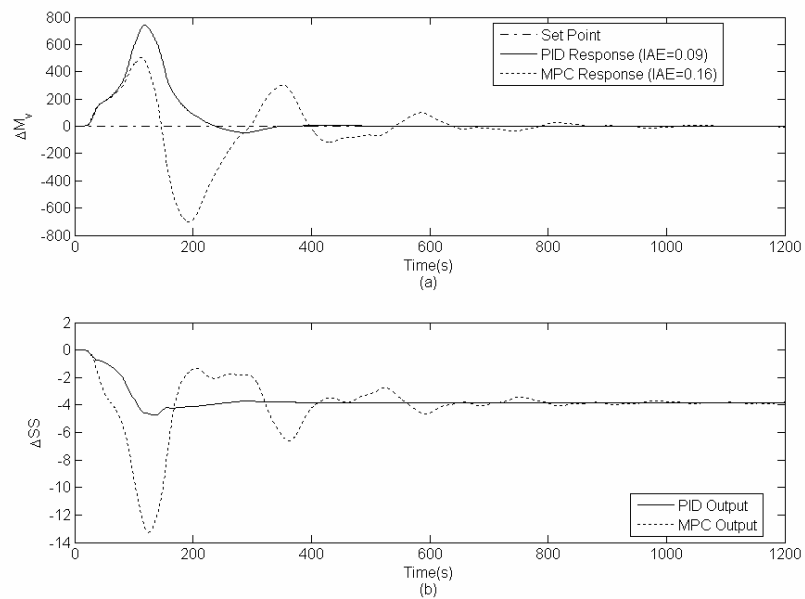


Figure 5.38: Disturbance rejection responses of PID and MPC (+10 °C step disturbance on T) (10% decrease in model gains).

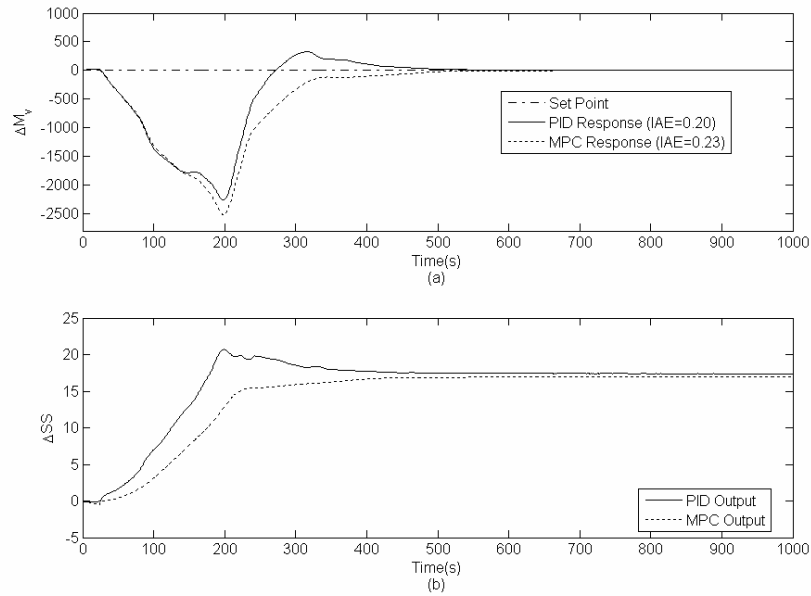


Figure 5.39: Disturbance rejection responses of PID and MPC (-10°C step disturbance on T) (10% decrease in model gains).

From Figures 5.30 to 5.39 and from Tables 5.13 and 5.14 it is seen that, both of the controllers are robust and are capable of eliminating the effects of disturbances and tracking the given set points even under the modeling errors.

Table 5.13: Normalized IAE scores and settling times of controllers in disturbance rejection performances (10% increase in model gains).

Case	MPC		PID	
	IAE Score	Settling Time	IAE Score	Settling Time
Positive Disturbance on FR	0.10	1200	0.07	500
Negative Disturbance on FR	0.24	650	0.17	650
Positive Disturbance on T	0.17	1500	0.08	550
Negative Disturbance on T	0.22	700	0.21	700

Table 5.14: Normalized IAE scores and settling times of controllers in disturbance rejection performances (10% decrease in models gains).

Case	MPC		PID	
	IAE Score	Settling Time	IAE Score	Settling Time
Positive Disturbance on FR	0.10	1200	0.08	600
Negative Disturbance on FR	0.29	800	0.20	650
Positive Disturbance on T	0.16	1200	0.09	600
Negative Disturbance on T	0.23	650	0.20	650

CHAPTER VI

CONCLUSIONS

In this study, experimental and theoretical studies are done to design an inferential control scheme for the feedback control of RPET degradation during extrusion process. The basic conclusions arrived are as follows:

- Degradation of PET is found to be highly nonlinear and it is affected by different variables such as barrel temperatures and residence time spent in the extruder.
- The product quality is considered to be determined by molecular weight, M_v , and can be measured indirectly by intrinsic viscosity ($[\eta]$).
- Dynamic experiments revealed that the extrusion process is highly nonlinear. It shows different behaviors for the positive or negative deviations of the inputs.
- Convolution models are selected to be the best and to be used in simulations rather than single or dual transfer functions of different properties.
- In the control system screw speed is evaluated to be manipulated variable using the SVD analysis while barrel temperature and feed flow rate left to be probable disturbances.
- In the control system designed, two different controllers (G_c^+ and G_c^-) are used for positive and negative parts of the process model.
- PID and MPC controllers' performances are found to be successful for set point tracking and disturbance rejection cases.
- PID and MPC controllers are proven to be robust under modeling errors ($\pm 10\%$).
- The designed inferential control scheme can be utilized in controlling the product quality in terms of molecular weight both with PID and MPC, once the off-line necessary data for the estimator is obtained.

REFERENCES

- Assadi, R., Colin, X., Verdu, J., (2004), "Irreversible structural changes during PET recycling by extrusion", *Polymer* 45, 4403-4412
- Awaja, F., Daver, F., (2004), "Recycled poly(ethylene terephthalate) chain extension by a reactive extrusion process", *Poly. Eng. Sci.* 44, 1579-1587
- Awaja, F., Dumitru, P., (2005), "Recycling of PET", *Eur. Polym. J.* 41, 1453-1477
- Bahar, A., Özgen, C., Leblebicioğlu, K., Halıcı, U., (2004), "Artificial neural network design for the inferential model predictive control of an industrial distillation column", *Ind. Eng. Chem. Res.* 43, 6102-6111
- Berkowitz, S., (1984), "Viscosity-molecular weight relationships for poly(ethylene terephthalate) in hexafluoroisopropanol-pentafluorophenol using SEC-LALLS", *J. App. Poly. Sci.* 29, 4353-4361
- Biagiola, S.I., Solsona, J.A., Figueroa, J.L., (2005), "Use of state estimation for inferential nonlinear MPC: a case study", *Chem. Eng. J.* 106, 13-24
- Brandrup, J., Immergut, E.H., (1989), "Polymer Handbook", 3rd Ed., Wiley Inc.
- Bregel, D., Seider, W.D., (1989), "Multistep nonlinear predictive controller", *Ind. Eng. Chem. Res.* 28, 1812-1822
- Broadhead, T.O., Patterson, W.I., Dealy, J.M., (1996), "Closed loop viscosity control of reactive extrusion with an in-line rheometer", *Polym. Eng. Sci.* 36, 2840-2851
- Camacho, E.F. and Bordons, C. (2000), "Model Predictive Control", Springer Verlag London Lim.
- Chelsea Center For Recycling And Economic Development (University of Massachusetts), (2000), "Potential end uses for polyester fiber waste: A laboratory study", Technical Report #33.
- Chen, Z.L., Chao, P.Y., Chiu S.H., (2003), "Proposal of an empirical viscosity model for quality control in the polymer extrusion process", *Polymer Testing* 22, 601-607
- Choulak, S., Couenne, F., Le Gorrec, Y., Jallut, C., Cassagnau, P., Michel, A., (2004), "Generic dynamic model for simulation and control of reactive extrusion", *Ind. Eng. Chem. Res.* 43, 7373-7382
- Costin, M.H., Taylor, P.A., Wright, J.D., (1982), "A critical review of dynamic modeling and control of plasticating extruders" *Polym. Eng. Sci.* 22, 393-401

- Costin, M.H., Taylor, P.A., Wright, J.D., (1982), "On the dynamics and control of a plasticating extruder", *Polym. Eng. Sci.* 22, 1095-1106
- De Ruyck, H., (1997), "Modeling of the residence time distribution in a twin screw extruder", *J. Food Eng.* 32, 375-390
- Doyle III, F.J., (1998), "Nonlinear inferential control for process applications", *J. Proc. Con.* 8 (5-6), 339-353
- Elsej, J., Reipenhausen, J., McKay, B., Barton, G.W., Willis, M., (1997), "Modeling and control of food extrusion process", *Computers Chem. Eng.* 21, s361-s366
- Fisher, E.G., (1976), "Extrusion of plastics", Hazell Watson And Viney Ltd.
- Garcia, C.E., Prett, D.M., Morari, M., (1989), "Model predictive control: Theory and practice – a survey", *Automatica* 25, 335-348
- Haley, T.A., Mulvaney S.J., (2000), "On-line system identification and control design of an extrusion cooking process: Part II. Model predictive and inferential control design", *Food Control* 11, 121-129
- Hassan, G.A., Parnaby, J., (1981), "Model reference optimal steady-state adaptive computer control of plastics extrusion process", *Polym. Eng. Sci.* 21, 276-284
- Incarnato, L., Scarfato, P., Di Maio, L., Acierno, D., (2000), "Structure and rheology of recycled PET modified by reactive extrusion", *Polymer* 41, 6825-6831
- Karayannidis P G. and Psalida E A., (2000), "Chain extension of recycled poly(ethylene terephthalate) with 2,2^F-(1,4-phenylene)bis(2-oxazoline)", *J. Appl. Polym. Sci.* 77, 2206-2211
- Kent, R.J., (1998), "Report 104: Plastics profile extrusion", *Rapra Review Reports*, Vol. 9 No.8
- Klema, V.C., Laub, A.J., (1980), "The singular value decomposition: Its computation and some applications", *IEEE Trans. Automatic Cont.* 25, 164-176
- Lee, S.J., Hong, C., Han, T., Kang, J., Kwon, Y.A., (2002), "Application of fuzzy control to start-up of twin screw extruder", *Food Control* 13, 301-306
- Luyben W.L., (1990), "Process modeling and control for chemical engineers", 2nd Ed., McGraw-Hill Book Co.
- Luyben, W.L., (2006), "Evaluation of criteria for selecting temperature control trays in distillation columns", *J. Proc. Cont.* 16, 115-134
- Marchetti, J.L., Mellichamp, D.A., Seborg, D.E., (1983), "Predictive control based on discrete convolution models", *In. Eng. Chem.* 22, 488-495
- Maurath, P.R., Mellichamp D.A., Seborg, D.E., (1988), "Predictive controller design for single-input/single-output (SISO) systems", *Ind. Eng. Chem. Res.* 27, 956-963

- Meziou, A.M., Deshpande, P.B., Cozewith, C., Silverman, N.I., Morrison, W.G., (1996), "Dynamic matrix control of an ethylene-propylene-diene polymerization reactor", *Ind. Eng. Chem. Res.* 35, 164-168
- Morningred, J.D., Paden, B.E., Seborg, D.E., Mellichamp, D.A., (1992), "An adaptive nonlinear predictive control", *Chem. Eng. Sci.* 47, 755-762
- Mudalamane, R., Bigio, D.I., (2003), "Process variations and the transient behavior of extruders", *AIChE J.* 49(12), 3150-3160
- Nied, S.A., Budman, H.M., Tzoganakis, C., (2000), "Control of a LDPE reactive extrusion process", *Cont. Eng. Prac.* 8, 911-920
- Obut, S., (2005), "Control of pH neutralization reactor of a waste water treatment system using identification reactor", M.Sc. Thesis, Chem. Eng Dept. METU
- Ogawa, M., Ohshima, M., Morinaga, K., Watanabe, F., (1999), "Quality inferential control of an industrial high density polyethylene process", *J. Proc. Con.* 9, 51-59
- Oromiehie, A., Mamizadeh, A., (2004), "Recycling PET beverage bottles and improving properties", *Polym. Int.* 53, 728-732
- Özkan. L., Kothare, M.V., Georgakis, C., (2003), "Control of solution polymerization reactor using multi-model predictive control", *Chem. Eng. Sci.* 58, 1207-1221
- Pabedinskas, A., Cluett, W.R., Balke, S.T., (1989), "Process control for polypropylene degradation during reactive extrusion", *Polym. Eng. Sci.* 29, 993-1003
- Parnaby, J., Kochhar, A. K., Wood, B., (1975), "Development of computer strategies for plastic extruders", *Polym. Eng. Sci.* 15, 594-605
- Pawlak, A., Pluta, M., Morawiec, J., Galeski, A., Pracella, M., (2000), "Characterization of scrap poly(ethylene terephthalate)", *Eur. Poly. J.* 36, 1875-1884
- PETCORE, <http://www.petcore.org>, last accessed on 7.8.2006
- Previdi, F., Savaresi, S.M., Panarotto, A., (2006), "Design of a feedback control system for real-time control of flow in a single-screw extruder", *Con. Eng. Prac.*, 14, 1111-1121
- Rauwendaal, C., (1998), "Understanding extrusion", Carl Hanser Verlag
- Rojas, O.J., Goodwin, G.C., Seron, M.M., Feuer, A., (2004), "An SCD based strategy for receding horizon control of input constrained linear systems", *Int. J. Robust Nonlinear Cont.* 14, 1207-1226
- Rosen, S.L., (1982), "Fundamental principles of polymeric materials", Wiley Inc.
- Seborg, D.E., Edgar, T.F., Mellichamp, D.A., (1989), "Process dynamics and control", Wiley Inc.
- Smith, J.M., Janssen, L.P.B.M., Koning, W.L., Abeln, P.P.J., (1978), "The operating characteristics of twin screw extruders", *Polym. Eng. Sci.* 18, 660-667

- Spinace, M.A., De Paoli, M.A., (2000), "Characterization of poly(ethylene terephthalate) after multiple processing cycles", *App. Poly. Sci.* 80, 20-25
- Stephanopoulos, G., (1984), "Chemical process control – an introduction to theory and practice", Prentice-Hall Inc.
- Tanrattanakul, V., Hiltner, A., Baer, E., Perkins, W.G., Massey, F.L., Moet, A., (1996), "Toughening PET by blending with a functionalized SEBS block copolymer", *Polymer* 38, 2191-2200
- Tanttu, J.T., Zchuchenko, A.I., Koivo, H.N., (1989), "A simulation study of the self-tuning control of a plastics extruder", *Control and Applications, ICCON, IEEE Int. Conf.*
- Torres, N., Robin, J.J., Boutevin B., (2000), "Chemical modification of virgin and recycled poly(ethylene terephthalate) by adding chain extenders during processing", *App. Poly. Sci.* 79, 1816-1824
- Wang, L. Gawthrop, P, Chessari, C., Podsiadly, T, Giles, A., (2004), "Indirect approach to continuous system identification of food extruder", *J. Pro. Cont.* 14, 603-615
- Wang, L., Chessari, C., Karpiel, E., (2001), "Inferential control of product quality attributes – application to food cooking extrusion process", *J. Proc. Con.* 11, 621-636
- Wang, Y., Tan, J., (2000), "Dual-target predictive control and application in food extrusion", *Cont. Eng. Prac.* 8, 1055-1062
- Wikipedia, http://en.wikipedia.org/wiki/Plastic_recycling, last accessed on 7.8.2006
- Wikipedia, http://en.wikipedia.org/wiki/Polyethylene_terephthalate, last accessed on 7.8.2006
- Wikipedia, http://en.wikipedia.org/wiki/Recycling_of_PET_Bottles, last accessed on 7.8.2006
- Wikipedia, http://en.wikipedia.org/wiki/Singular_value_decomposition, last accessed on 8.2.2006
- Xanthos, M., (1992), "Reactive extrusion – principles and practice", Carl Hanser Verlag
- Xiao, K., Tzoganakis, C., Budman, H., (2001), "Control of coating properties of LDPE through melt strength measurements", *Cont. Eng. Prac.* 9, 357-366
- Yang, B., Lee, L.J., (1986), "Process control of polymer extrusion. Part I: Feedback control", *Polym. Eng. Sci.* 26, 197-204
- Zheng, D., Hoo, K.A., (2004), "System identification and model-based control for distributed parameter systems", *Comp. Chem. Eng.* 28, 1361-1375

APPENDIX A

MOLECULAR WEIGHT DETERMINATION

Viscosities¹ of polymer solutions are usually measured in glass viscometers (Figure D.1), in which the solution flows through a capillary tube by gravity. Two common types are Ostwald and Ubbelohde viscometers. The Ubbelohde viscometer has the advantage that the flowing solution is not affected by the amount of the liquid in the reservoir. Thus, the concentration of the solution can be changed directly in the viscometer.

A.1 Molecular Weight Determination

The molecular weights (M_v) of the collected samples are determined by *dilute solution viscometry*, using a *Ubbelohde* type viscometer.

0.06 gram of sample is weighted and dissolved in 6 ml of trifluoroacetic acid (TFA) in a test tube, giving 1 g/dl concentration.

Initially, the flow time of pure solvent (t_0) between two mark points is measured using a chronometer, and recorded. The initial amount of pure solvent (TFA) in the viscometer is 7 ml. Measurement of t_0 is repeated until same 'minute:second' value is read with the previous flow (or flow time became constant).

¹ "Since polymer solutions are non-Newtonian, intrinsic viscosity must be defined, strictly speaking, in terms of the zero-shear or lower Newtonian viscosity. This is rarely a problem because the low shear rates in the usual glassware viscometers give just that. Occasionally, however, extrapolation to zero-shear condition is required" [Rosen, 1982].

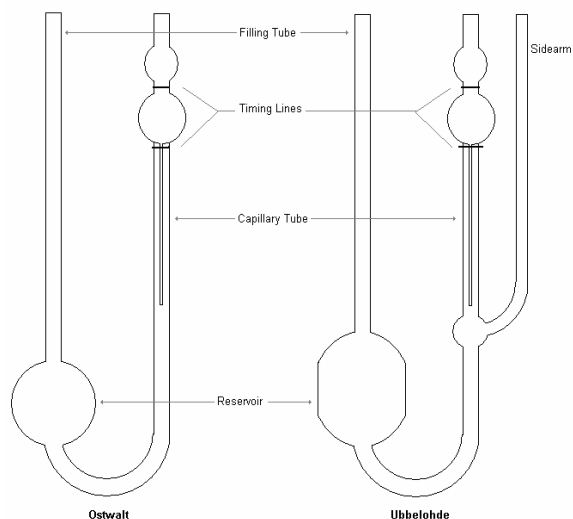


Figure A.1: Ostwald and Ubbelohde viscometers.

When the flow time of pure solvent (t_0) got constant in means of seconds, 1 ml of RPET-TFA solution is added from the test tube to the viscometer, and the flow time of this new concentration (t_1) is measured, again until it got constant in means of seconds.

Above step is repeated 4 times (t_1, t_2, t_3, t_4) (see Appendix E). Using these flow times, values for reduced viscosity (η_{red}) were calculated and plotted against corresponding concentration ($[C]$) values. Then the *best line (trend line)*¹ passing through these points is calculated and its intercept at zero concentration is taken as *intrinsic viscosity* ($[\eta]$). After the intrinsic viscosity value was obtained, Equation A.1 is used to calculate the M_v of the sample.

$$M_v = \left(\frac{[\eta]}{K} \right)^{\frac{1}{\alpha}} \quad (\text{A.1})$$

Symbols K and α refer to the *Mark Hauwing* constants for PET-TFA solution.

¹ For any sample, when the 'reduced viscosity' was plotted against 'concentration', if the R^2 value for the best line (trend line) was below 0.98 that molecular weight determination was repeated for that sample. By this way, the experimental errors were tried to be kept at minimum.

APPENDIX B

CALIBRATION FOR RESIDENCE TIME AND FEED RATE

B.1 Residence Time

Average residence time (ART) measurements for the studied screw speeds are given in Table B.1. Same ART values were measured for different feed rates, as pointed in the literature [Xanthos, 1992].

Table B.1: Average residence times for studied screw speeds.

Screw speed (rpm)	Residence time (second)
50	255
125	137
200	122
275	115
350	15
425	13
500	11

In Figure B.1, it is seen clearly that ART changes in steps for screw speed. In other words, for a range of screw speed values, ART remains almost unchanged.

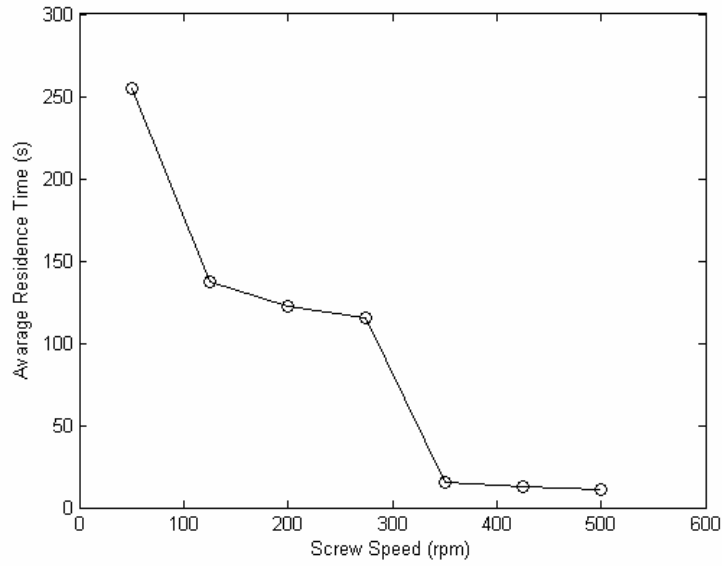


Figure B.1: Average residence times measured at different screw speeds.

B.2 Feed Rate

The extruder control panel had the feed rate (FR) setting between the values of 0 and 999. Thus, the feed rate and corresponding flow rate (g/min) values needed to be calibrated. The calibration data for studied feed rate settings is given in Table B.2.

Table B.2: Flow rate calibration data for studied feed rate settings.

Feed rate reading	Flow rate (g/min)
25	3.85
50	5.70
75	7.12
100	8.16

Figure B.2 shows that the relation between the FR and corresponding flow rate can be accepted as linear.

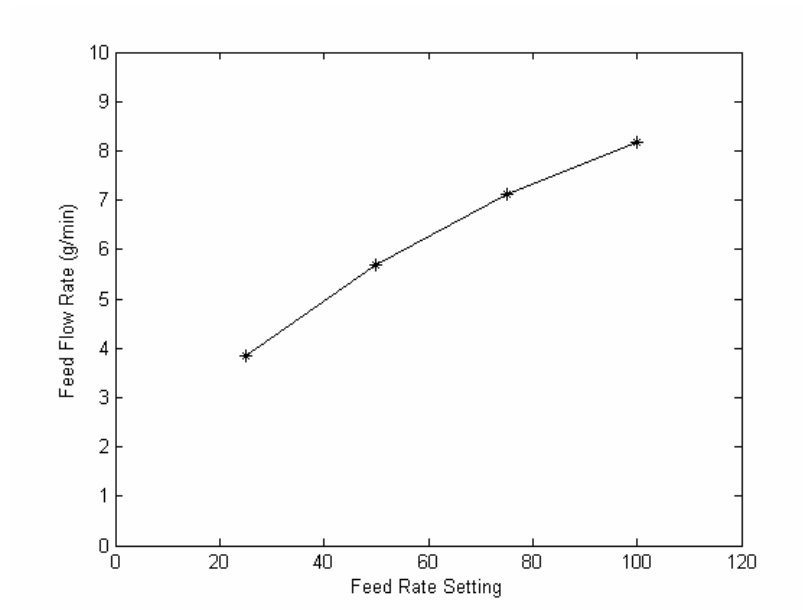


Figure B.2: Feed rate settings and corresponding flow rates (g/min).

APPENDIX C

EXPERIMENTAL DATA

Table C.1: Molecular weight (g/gmol), M_v , change for different SS and FR values at 270 °C.

FR	Screw Speed (rpm)						
	50	125	200	275	350	425	500
25 (3.85 g/min)	7769	7873	10549	9268	10352	6313	9788
50 (5.70 g/min)	8361	669	12786	12769	6679	9828	12652
75 (7.12 g/min)	1696	14053	11741	5924	6183	10265	12665
100 (8.16 g/min)	12521	12226	9467	9146	13177	10221	11966

Table C.2: Molecular weight (g/gmol), M_v , change for different SS and FR values at 290 °C.

FR	Screw Speed (rpm)						
	50	125	200	275	350	425	500
25 (3.85 g/min)	6689	8774	12239	8520	9194	9913	7322
50 (5.70 g/min)	8642	10234	8416	10804	13042	13344	9587
75 (7.12 g/min)	10259	13103	10965	5932	8120	9748	10436
100 (8.16 g/min)	6809	9506	8572	6949	8355	10744	11310

Table C.3: Molecular weight (g/gmol), M_v , change for different SS and FR values at 310 °C.

FR	Screw Speed (rpm)						
	50	125	200	275	350	425	500
25 (3.85 g/min)	4504	3487	5507	2024	4805	5101	5584
50 (5.70 g/min)	7125	6121	7082	8642	7995	8956	5790
75 (7.12 g/min)	6034	11201	6890	9116	7218	6049	8680
100 (8.16 g/min)	9244	9250	7708	9331	6876	9346	7358

Table C.4: M_v (g/gmol) change with SS, FR and T (dynamic runs).

Time (s)	SS Plus Step (25 rpm)	SS Minus Step (50 rpm)	FR Plus Step (1.04 g/gmol)	FR Minus Step (1.42 g/gmol)	T Plus Step (20 °C)	T Minus Step (20 °C)
0	11546	11301	11300	11300	11300	11500
10			11375	11371		
20	10810	11051			11310	11555
30			11546	10505		
40	10965	10445			11611	11042
50			11718	10271		
60	11156	7969			11750	10520
70	11617		11868	9877		
80	12200	6279			12019	9947
90	12495		12137	8610		
100	12961	5405			12658	8977
110	13457		12382	7885		
120	13928	3844		7618	13079	8511
130	14694		12548	5289		
140	14388	3601		2576	13008	8015
150	14140		12538	1275		
160	14106	2449		973	12675	7657
170			12495	1500		
180		2147		2207	12632	6936
190				2259		
200		1466			12628	5972
210						
220		1764				7136
230						
240		1796				8203
250						
260		1696				8280
270						
280						8292

APPENDIX D

PID CONTROL LOOP AND PROGRAM CODES

PID control loop designed using SIMULINK is given in Figure D.1.

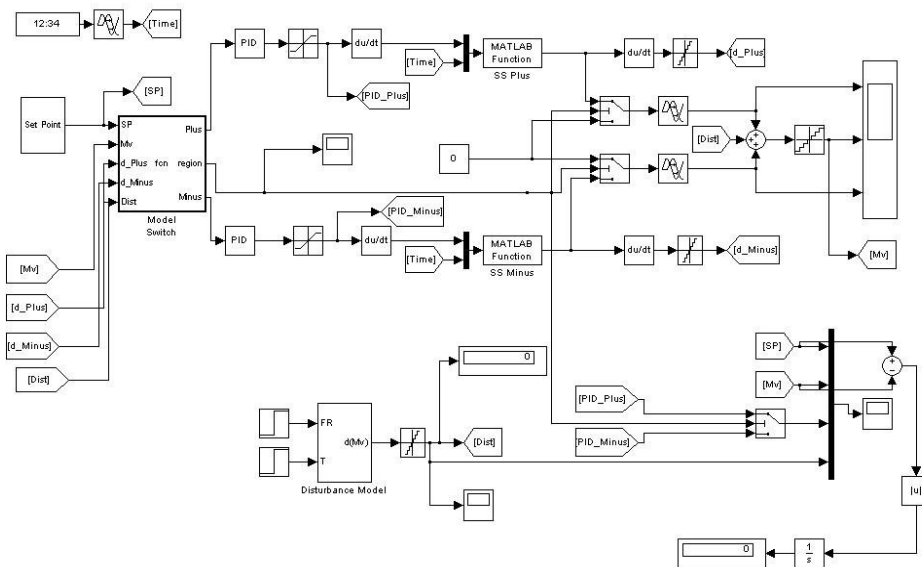


Figure D.1: Feedback control loop for PID controllers designed in SIMULINK.

Code for the 'SS⁺ Model' is given below as an example for all positive and negative models.

```
% Screw Speed Dynamic Model (Positive Part)

function [ c_t_SS_Positive ] = SS_Positive_func(input)

delta_input = input(1);
delta_time = input(2);

try a_SS_Positive=evalin('base','a_SS_Positive'); catch a_SS_Positive = [];
```

```

end;
try delta_m_SS_Positive=evalin('base','delta_m_SS_Positive'); catch
delta_m_SS_Positive = []; end;

model=evalin('base','SS_Positive_Fit');

n = delta_time+1;

a_SS_Positive(n) = model(delta_time);
delta_m_SS_Positive(n) = delta_input;

if n >=2
    count = numel(a_SS_Positive);
    a_vector = a_SS_Positive(2:count);
    m_vector = delta_m_SS_Positive((count-1):-1:1);
    summation = a_vector.*m_vector;
    c_t_SS_Positive = sum(summation);
else
    c_t_SS_Positive = 0;
end

assignin('base','a_SS_Positive',a_SS_Positive);
assignin('base','delta_m_SS_Positive',delta_m_SS_Positive);

```

Code of the model predictive control part is given below.

```

% MPC code

clc;clear

addpath Source;
load Fitted_Models;
load MPC_Positive_Minus;

Stop_Time          = 500;          %Total Simulation Time

delta_input        = 0;            %maginitude of delta input
delta_input_time   = 0;            %time of delta input

Set_Points         = [0 0 -10 0]; % Set Point(s) vector with 'n' elements
Set_Point_times    = [0 1000 2000 3000]; % Set Point Time(s) vector with 'n'
                                         elements

%Disturbance Types -> (0) None || (1) FR Positive || (-1) FR Minus || (2) T Positive
|| (-2) T Minus
Dist_Type          = 0;
Dist_Magnitude     = 0;
Dist_Time          = 0;

% Initial Values

MPC_Positive_state = mpcstate(MPC_Positive);
MPC_Minus_state   = mpcstate(MPC_Minus);

u = 0;
u_prev = 0;
du = 0;

d_Positive = 0;
d_Minus = 0;
Mv_t = 0;

Dist_prev = 0;

% Simulation starts here
for time = 0:1:Stop_Time

```

```

for sp_detect = 1:numel(Set_Point_times) % Follow Set Points
    if time == Set_Point_times(sp_detect)
        Set_Point = Set_Points(sp_detect);
    end
end

if not(Dist_Type == 0); % Disturbance Part
    if time >= Dist_Time
        dist_delta_time = time - Dist_Time;
        Dist_delta_u = Dist_Magnitude - Dist_prev;
        Mv_dist = disturbance_func(dist_delta_time,Dist_Type,Dist_delta_u);
        Dist_prev = Dist_Magnitude;
    else
        Mv_dist = 0;
    end
else
    Mv_dist = 0;
end

region = region_select(d_Positive,d_Minus,Mv_t,Set_Point,Mv_dist);

switch region
case 0, % No models need to run
case 1, % SP Positive Region

    clear minus_start_time

    try Positive_start_time;
    catch Positive_start_time = time;
    end

    u = mpcmove(MPC_Positive, MPC_Positive_state,Mv_t,Set_Point,[]);

    du = u - u_prev;
    Mv_t_prev = Mv_t;

    delta_time = time - Positive_start_time;

    Mv_t_Positive = SS_Positive_func([du delta_time]);

    Mv_t = Mv_t_Positive + Mv_dist;

    u_prev = u;
    d_Positive = Mv_t - Mv_t_prev;

    if abs(d_Positive) < 0.000001
        d_Positive = 0;
    end

    if abs(Mv_t) < 0.1
        Mv_t = 0;
    end

    assignin('base','Positive_start_time',Positive_start_time);

case -1, % SP Minus Region

    clear Positive_start_time

    try minus_start_time;
    catch minus_start_time = time;
    end

    u = mpcmove(MPC_Minus,MPC_Minus_state,Mv_t,Set_Point,[]);

    du = u - u_prev;
    Mv_t_prev = Mv_t;

    delta_time = time - minus_start_time;

    Mv_t_minus = SS_Minus_func([du delta_time]);

```

```

Mv_t = Mv_t_minus + Mv_dist;

u_prev = u;
d_Minus = Mv_t - Mv_t_prev;

if abs(d_Minus) < 0.000001
    d_Minus = 0;
end

if abs(Mv_t) < 0.1
    Mv_t = 0;
end

assignin('base','minus_start_time',minus_start_time);

case 10,                % Disturbance Positive Region
case -10,               % Disturbance Minus Region
end

Mv_hist(time+1) = Mv_t;
Mv_dist_hist(time+1) = Mv_dist;
u_hist(time+1) = u;
du_hist(time+1) = du;
SP_hist(time+1) = Set_Point;
region_hist(time+1) = [region];

MPC_Dist_Response(time+1,:) = [time Set_Point Mv_dist Mv_t u];

end

disp 'finished'
subplot(2,1,1);plot(Mv_hist,'k');hold on;plot(SP_hist,':r');plot(Mv_dist_hist,'r');
subplot(2,1,2);plot(u_hist)

figure
plot(region_hist)

```

APPENDIX E

SAMPLE CALCULATIONS

E.1 Molecular Weight Calculations

In Table E.1 an example of the experimental data collected during the viscosity measurements are given.

Table E.1: Experimental data (an example).

Sample: steady-state experiments (T: 290 °C, FR: 25, SS: 50 rpm)			
0.0630 grams sample + 6 ml TFA			
Solution in reservoir	t_n	Measured flow times (min.sec.milisc)	Constant flow time (sec)
Pure Solvent{7 ml}	t_0	1) 2.28.12 2) 2.28.26	148
+ 1 ml addition	t_1	1) 2.37.91 2) 2.37.57	157
+ 1 ml addition	t_2	1) 2.47.31 2) 2.46.72 3) 2.47.09	166
+ 1 ml addition	t_3	1) 2.55.38 2) 2.55.88	175
+ 1 ml addition	t_4	1) 3.03.16 2) 3.02.56 3) 3.02.17	182
+ 1 ml addition	t_5	1) 3.09.72 2) 3.09.19	189

Using the measured flow times, calculations are done and results are given in Table E.2.

Table E.2: Reduced viscosity for different concentrations.

n	Flow time of solution (t_0)	Relative viscosity $\eta_{rel} = \frac{t_n - t_0}{t_0}$	Concentration in reservoir [C]	Reduced Viscosity $\eta_{red} = \frac{\eta_{rel}}{[C]}$
0	148	0	0.0000	-
1	157	0.061	0.131	0.463
2	166	0.122	0.233	0.521
3	175	0.182	0.315	0.579
4	182	0.230	0.382	0.602
5	189	0.277	0.438	0.633

The calculated values for reduced viscosity (η_{red}) were plotted against corresponding concentration ([C]) values, as illustrated in Figure E.1. Then the best line (trend line) passing through these points was calculated and its intercept at zero concentration was taken as intrinsic viscosity ($[\eta]$).

The viscosity average molecular weight (M_v) is calculated using Equation E.1.

$$M_v = \left(\frac{[\eta]}{K} \right)^{\frac{1}{\alpha}} \quad (E.1)$$

$$M_v = \left(\frac{0.393}{1.4 \times 10^{-3}} \right)^{1.5625} = 6689.8 \frac{g}{mol}$$

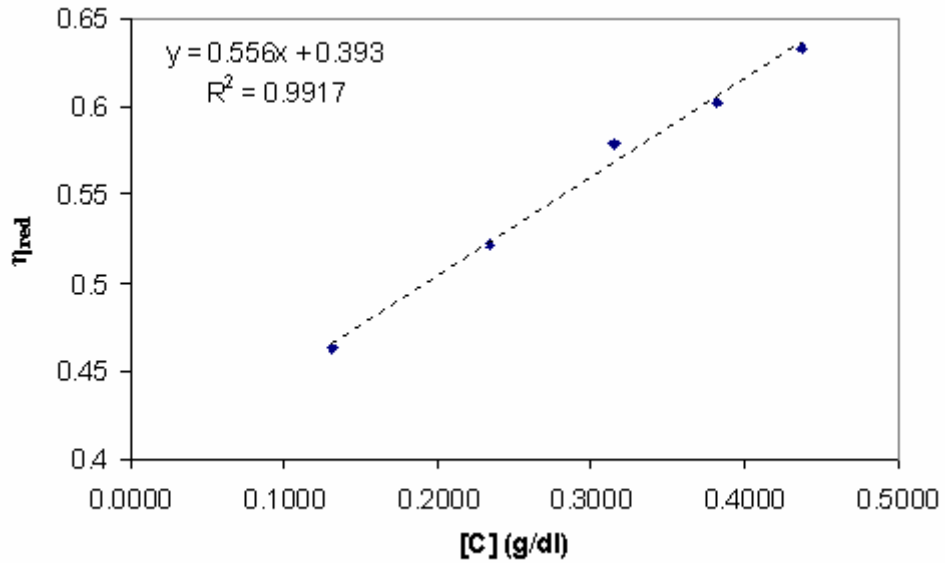


Figure E.1: Reduced viscosity change with concentration.

E.2 PID TUNING CALCULATIONS

The PID controllers studied are first tuned by *modified Ziegler-Nichols method* as given in the literature [Seborg et al., 1989]. They are then further fine tuned by trial-error procedure.

Table E.3 gives the *ultimate gains* (K_u) and the *ultimate periods* (P_u) of the continuous oscillations for the positive and negative PID-model pairs.

Table E.3: Ultimate gains and ultimate periods of positive and negative PID-model pairs.

Pair	K_u (rpm.gmol/g)	P_u (seconds)
PID ⁺ -SS ⁺	0.00748	182
PID ⁻ -SS ⁻	0.0174	112

The relations between the K_u and P_u and the PID parameters (K_c, τ_i, τ_D) are given in Table E.3.

Table E.4: Original and modified Ziegler-Nichols settings for PID controllers [Seborg et al., 1989].

	K_c	τ_i	τ_D
Original (1/4 decay ratio)	$0.6K_u$	$P_u/2$	$P_u/8$
Some Overshoot	$0.33K_u$	$P_u/2$	$P_u/3$
No Overshoot	$0.2K_u$	$P_u/2$	$P_u/3$